INTERNATIONAL ATOMIC ENERGY AGENCY
UNITED NATIONS EDUCATIONAL, SCIENTIFIC AND CULTURAL ORGANIZATION
INTERNATIONAL CENTRE FOR THEORETICAL PHYSICS
I.C.T.P., P.O. BOX 586, 34100 TRIESTE, ITALY, CABLE: CENTRATOM TRIESTE

UNITED NATIONS INDUSTRIAL DEVELOPMENT ORGANIZATION
INTERNATIONAL CENTRE FOR SCIENCE AND HIGH TECHNOLOGY
c/o INTERNATIONAL CENTRE FOR THEORETICAL PHYSICS 34100 TRIESTE (ITALY) VIA GRIGNANO, 9 (ADRIATICO PALACE) P.O. BOX 586 TELEPHONE (040) 224572 TELEFAX (040) 224575 TELEX 460449 APH I

SMR/543 - 13

EXPERIMENTAL WORKSHOP ON HIGH TEMPERATURE SUPERCONDUCTORS AND RELATED MATERIALS (BASIC ACTIVITIES)

(11 February - 1 March 1991)

" Magnetic Flux Behaviour in High- (and Low-) T_c Superconductors "

presented by:

D.O. WELCH
Brookhaven National Laboratory
Materials Science Division
Upton, NY 11973
U.S.A.

For distribution to participants

Magnetic Flux Behavior in High- (and Low-) T_c Superconductors

David O. Welch
Materials Science Division
Brookhaven National Laboratory
Upton, NY 11973, USA

- 3 lectures : basic ideas, overview
  - reversible properties
  - irreversible properties

Some Useful References

- A.C. Rose-Innes & E.H. Roderick, *Introduction to Superconductivity*, [Pergamon, Oxford 1969]
- M. Tinkham, *Introduction to Superconductivity*, [McGraw-Hill, New York, 1975]
- R.P. Huebner, *Magnetic Flux Structures in Superconductors*, [Springer-Verlag, Berlin, 1979]
- M. Tinkham and C.J. Lobb, "Physical Properties of the New Superconductors," Solid State Physics, Vol. 42 (1989)
- R. Dolven, "Physics of the critical magnetic field in type-II superconductors," Am. J. Phys. 52, 1093 (1984)
- J.R. Clem
  - "Phenomenological theory of magnetic structure in the high-temperature superconductors," Proc. M^2S-HTSC Conf., Stanford, CA July 23-28, 1989 special issue Physica C (1989)
  - "Magnetic properties of the high-temperature superconductors," in *Physics and Materials Science of High-Temperature Superconductors*, R. Kossowsky et al., Eds. (Kluwer Academic Publishers, Dordrect, 1990) p. 79

REFERENCES, CONT.

- J.R. Clem, cont.
  - "Magnetic flux transport in superconductors," in Proc. Int'l. Conf. on Transport Properties of Superconductors, ICTPS '90, Rio de Janeiro, Brazil, Apr 29 - May 5, 1990; R. Nicolsky, ed. (World Scientific, Singapore)

- L.J. Campbell, M.M. Doria, V.G. Kogan, "Vortex lattice structures in uniaxial superconductors," Phys. Rev. B 38, 2939 (1988).

- G.J. Dolan, et al., "Vortex structure in $YBa_2Cu_3O_7$ and Evidence for intrinsic pinning," Phys. Rev. Lett. 62, 827 (1989)

- D.R. Nelson, "Vortex entanglement in high-T_c superconductors," Phys. Rev. Lett. 60, 1973 (1988)

- D.S. Fisher, M.P.A. Fisher and D.A. Huse, "Thermal fluctuations, quenched disorder, phase transitions, and transport in type-II superconductors," Phys. Rev. B 43, 130 (1991)

- S.P. Obukhov and M. Rubinstein, "Topological gloss transition in entangled flux state," Phys. Rev. Lett. (1990)

- A. Barone, A.I. Larkin, Y.N. Ovchinnikov, "Vortices in layered superconductors," J. Supercond. 3, 155 (1990)

REFERENCES, Cont.

- C.P. Bean, Phys. Rev. Lett. 8, 250 (1962)
  Introduction of Critical State Model

- B. Oh et al., Appl Phys. Lett. 51, 852 (1987)
  Experimental justification of Bean model for 1-2-3 films

- Martin Wilson, Superconducting Magnets, Oxford U. Press. Shows how to make good use of critical state model.

- J. Orehotsky et al, "60-Hz ac losses in $YBa_2Cu_3O_7$ cylinders," J. Appl. Phys. 63, 1133 (1990)

- K.H. Müller, "Frequency dependence of ac susceptibility in high-temperature superconductors: flux creep and critical state at grain boundaries," Physica C 168, 585 (1990).

- E.H. Brandt, "Rigid levitation and suspension of high-temperature superconductors by magnets," Am. J. Phys. 58, 43 (1990)

- Fluctuation, "Melting," Depinning, Creep, and Diffusion of the flux-line lattice in high-T_c superconductors," Proc. Conf. on Low Temp Physics LT19, Physica B (in press)

References, cont.

- P.H. Kes and J. van den Berg, "Flux pinning and thermally activated depinning in single crystals of high-Temp. superconductors," in Studies of High Temperature Superconductors, A.V. Narlikar, ed., Nova Science Publishers, Commack, NY, USA
- M.R. Beasley, R. Labusch, W.W. Webb, Phys. Rev. 181, 682 (1969)
- Y. Xu, M. Suenaga, A.R. Moodenbaugh, D.O. Welch, Phys. Rev. B 40, 10822 (1989)
- D.O. Welch, Proc. Applied Superconductivity Conf. 1990, IEEE Transactions on Magnetics, March 1991, in press.
- R. Griessen et al:
  - Phys. Rev. Lett 62, 2857 (1989)
  - Phys. Rev. Lett 64, 1674 (1990)
  - Physica C 157, 199 (1989)
- M.V. Feigel'man, V.B. Geshkenbein, and A.I. Larkin, Physica C 167, 177 (1990)

Why Do We Care About Magnetic Flux Behavior?

- Science of Superconductivity

  e.g. Meissner effect, Type I vs Type II behavior, flux quantization ....

- Applications

  e.g. flux pinning, Josephson junctions, SQUIDs, flux-flow devices, Abrikosov memories, ...

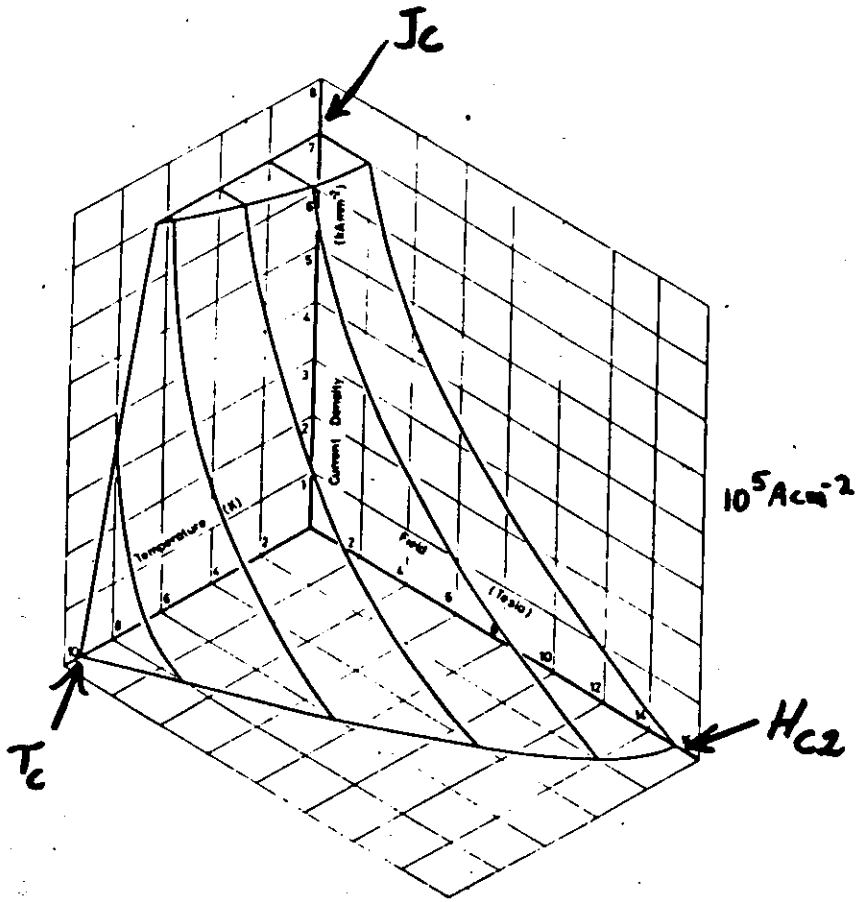

Fig. 1.1 Critical-current surface for a commercial superconducting alloy of niobium–titanium. (Based on recent measurements at 4.2 K, together with earlier measurements at variable temperature by Hampshire, R., Sutton, J., and Taylor, M. T. (1969).)

Although it is possible to make high-T_c superconductors in various forms by various methods, they cannot be used in magnets, power transmission lines, or even microelectronics unless the critical current density J_c is $10^5 - 10^6$ A cm^{-2}

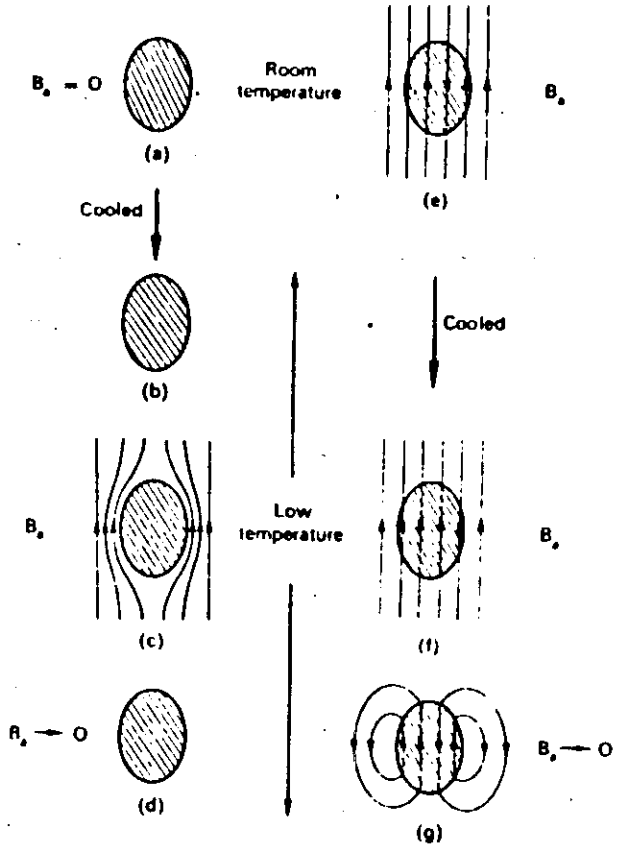

FIG. 2.2. Magnetic behaviour of a "perfect" conductor. (a)–(b) Specimen becomes resistanceless in absence of field. (c) Magnetic field applied to resistanceless specimen. (d) Magnetic field removed.

(e)–(f) Specimen becomes resistanceless in applied magnetic field. (g) Applied magnetic field removed.

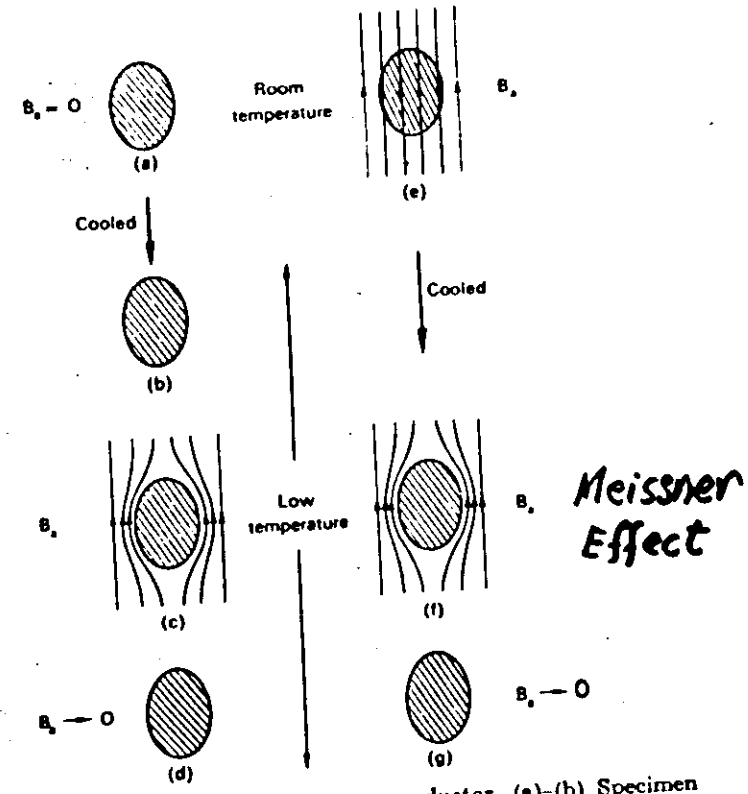

Meissner Effect

FIG. 2.3. Magnetic behaviour of a superconductor. (a)–(b) Specimen becomes resistanceless in absence of magnetic field. (c) Magnetic field applied to superconducting specimen. (d) Magnetic field removed.

(e)–(f) Specimen becomes superconducting in applied magnetic field. (g) Applied magnetic field removed.

PHENOMENOLOGICAL

THEORETICAL FRAMEWORK FOR UNDERSTANDING MAGNETIC EFFECTS IN SUPERCONDUCTORS

- MAXWELL'S EQUATIONS

$$\downarrow$$

$$\frac{\partial \vec{B}}{\partial t} = -\nabla \times \vec{E}$$

$$\nabla \times \vec{B} = \mu_0 \vec{J}_s$$

F=ma → $$\frac{\partial \vec{J}_s}{\partial t} = \frac{n_s e^2}{m} \vec{E}$$

$$\Big\} \quad \nabla^2\left(\frac{\partial \vec{B}}{\partial t}\right) = \frac{1}{\lambda_L^2} \frac{\partial \vec{B}}{\partial t}$$

↑ describes behavior of a perfect conductor

$$\dot{B} = \dot{B}_0 e^{-x/\lambda_L}$$

INSIDE PERFECT CONDUCTOR FLUX DENSITY DOES NOT CHANGE WITH TIME

- LONDON EQUATIONS

MEISSNER EFFECT:

A SUPERCONDUCTOR IS A PERFECT DIAMAGNET FOR LOW FIELDS, NOT JUST A PERFECT CONDUCTOR

$$\therefore \nabla^2 B = \frac{1}{\lambda_L^2} B$$

TWO-FLUID PICTURE

- TWO INTERPENETRATING FLUIDS BELOW T_c

Superfluid + normal fluid: $\vec{J} = \vec{J}_s + \vec{J}_N$

condensate of paired electrons (Cooper pairs in BCS); highly coherent, rigid wave function; screens applied E & H non-resistively

both of thermally excited quasi-particles contributes to entropy, sp. ht, thermal cond., ultrasonic attn., surface resistance

COHERENCE LENGTH ξ

- NORMAL FLUID OBEYS MAXWELL'S EQNS. AND OHM'S LAW: $\vec{J}_N = \sigma' \vec{E}$ OHM'S LAW

- SUPERFLUID OBEYS LONDON EQNS.:

$$\nabla \times \vec{J}_s = -\frac{1}{\mu_0 \lambda_L^2} \vec{B}$$ PERFECT DIAMAGNETISM

$$\frac{\partial \vec{J}_s}{\partial t} = \frac{1}{\mu_0 \lambda_L^2} \vec{E}$$ PERFECT CONDUCTIVITY

WHERE:

$$\lambda_L^2 = \frac{m}{\mu_0 e^2 n_s}$$

λ_L: LONDON PENETRATION DEPTH

n_s: DENSITY OF SUPERFLUID ELECTRONS

Important Length Scales in Superconductors

- magnetic penetration depth λ

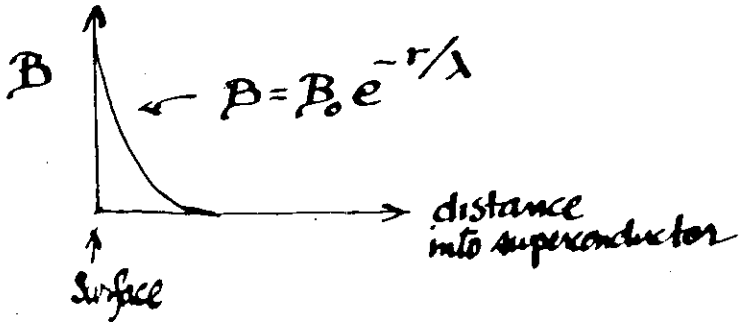

- coherence length ξ

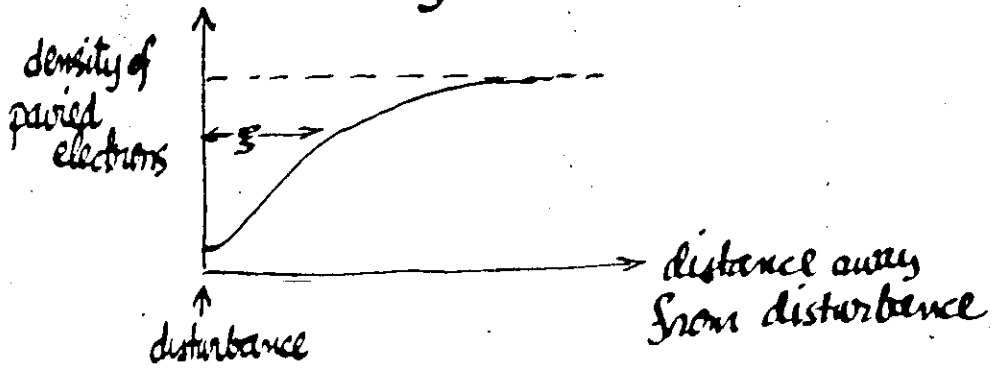

EXAMPLE: Superconducting Slab in a Parallel Magnetic Field

- $\nabla^2 B = -\frac{B}{\lambda_L^2}$

$$\Downarrow$$

$$\vec{B} = B_z(x)\,\vec{e}_z \quad \text{where} \quad B_z(x) = \mu_0 H_a \frac{\cosh\left(\frac{x}{\lambda_L}\right)}{\cosh\left(\frac{a}{\lambda_L}\right)}$$

- $\nabla \times \vec{B} = \mu_0 \vec{J}_s$

$$\Downarrow$$

$$-\frac{\partial B_z(x)}{\partial x} = \mu_0 J_{s,y} \quad \text{or} \quad J_{s,y} = \frac{H_a}{\lambda_L} e^{-\frac{x}{\lambda_L}}$$

THE APPLIED FIELD INDUCES A SCREENING CURRENT WHICH DIES OUT IN A PENETRATION DEPTH

Magnetization:

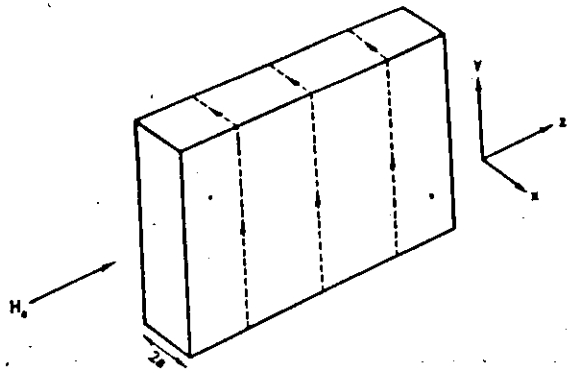

FIG. 8.1. Superconducting plate of thickness $2a$ with a magnetic field parallel to its surfaces. Its length and height are assumed much greater than $2a$. The broken lines show the direction of the screening currents.

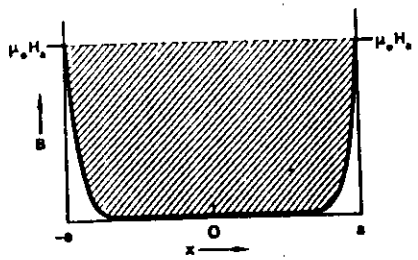

FIG. 8.2. Variation of B with distance normal to the surface for a plate of thickness $2a$ ($2a \gg \lambda$). The cross-hatched area is proportional to the magnetic moment and to the magnetic free energy.

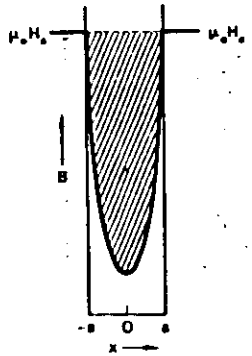

e.g. fine-grained s.c. oxide

FIG. 8.3. Variation of B with distance normal to the surface for a plate of thickness $2a$ ($a \sim \lambda$).

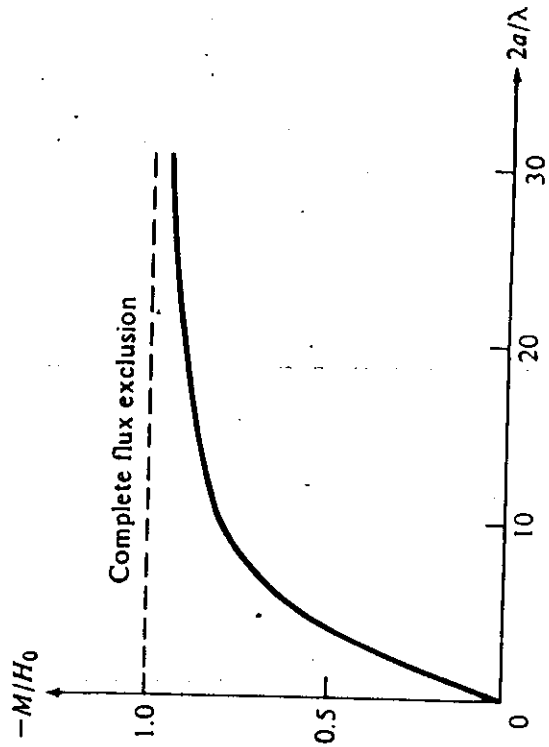

Figure 6.05c. Average magnetization in the superconducting slab in Fig. 6.05b as a function of slab thickness, normalized to the penetration depth. It is common convention to consider the magnetization to be negative if it is directed in the direction opposite to the applied magnetic field.

For
High-T_c Oxide Single Crystals:

ANISOTROPIC EFFECTIVE MASS THEORY

(John Clem, V. Kogan, ...

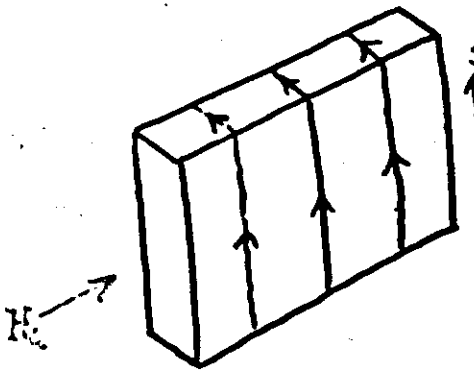

principal axes of crystal

$$\lambda_i = \lambda\sqrt{m_i} \qquad \text{where } m_1 m_2 m_3 = 1$$

λ_i: decay length of (super-)current flowing along the i axis

For $YBa_2Cu_3O_7$: $\lambda_a : \lambda_b : \lambda_c = 1.2 : 1 : 5.5$

(λ_b: direction of CuO chains)

For $Bi_2Sr_2CaCu_2O_{8+\delta}$: $\lambda_a : \lambda_b : \lambda_c \cong 1 : 1 : 55$

Screening Currents

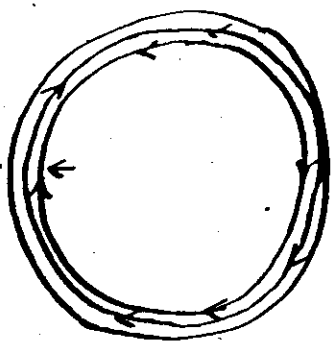

λ_L → penetration depth

"good" superconductor
e.g. ideal single crystal of superconducting oxide
$\lambda_L(T=0) \simeq 1\text{-}2 \times 10^3$ Å
low T_c polycrystalline Nb_3Sn ...

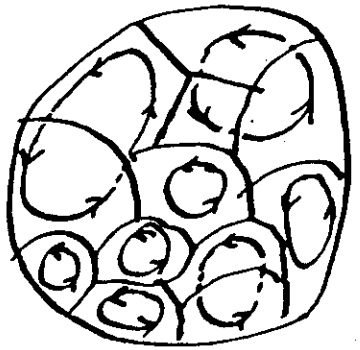

granular superconductor
e.g. polycrystalline oxide, real single crystal in magnetic field, ...

also:
muon spin rotation
neutron scattering

Measurement of λ using frequency of CR-L circuit containg the superconductor inside a coil.

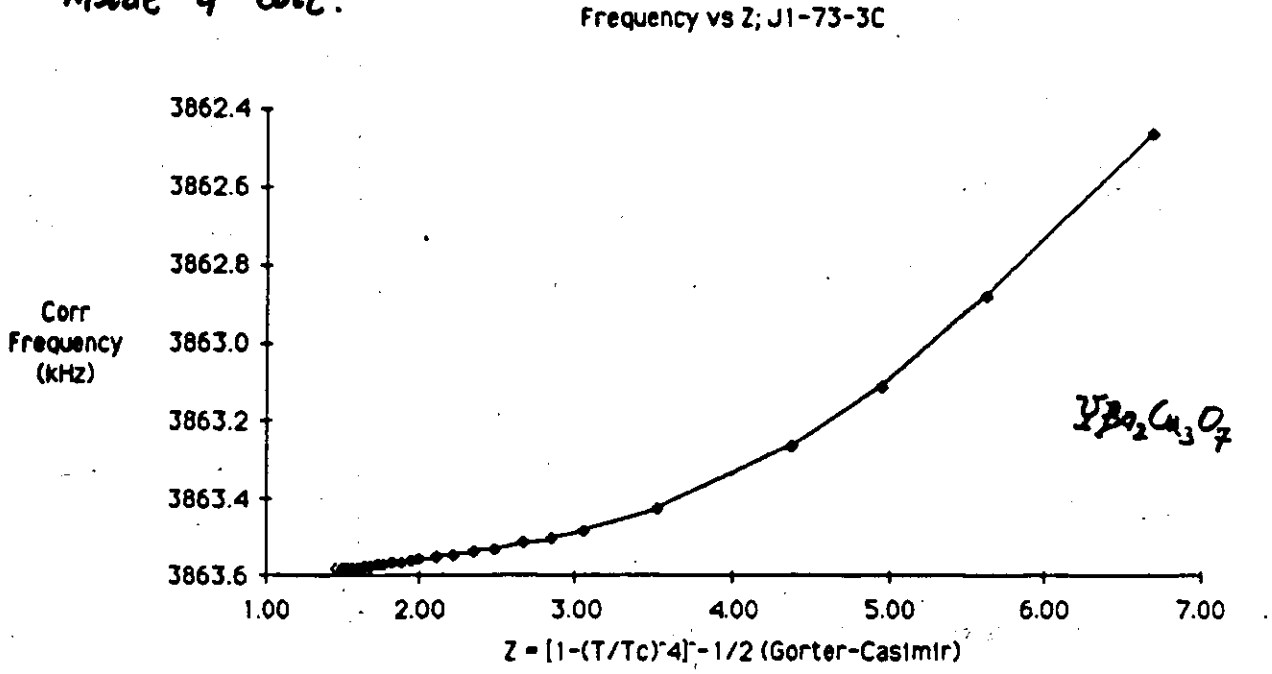

$$\frac{1}{(1-(T/T_c)^4)^{1/2}}$$

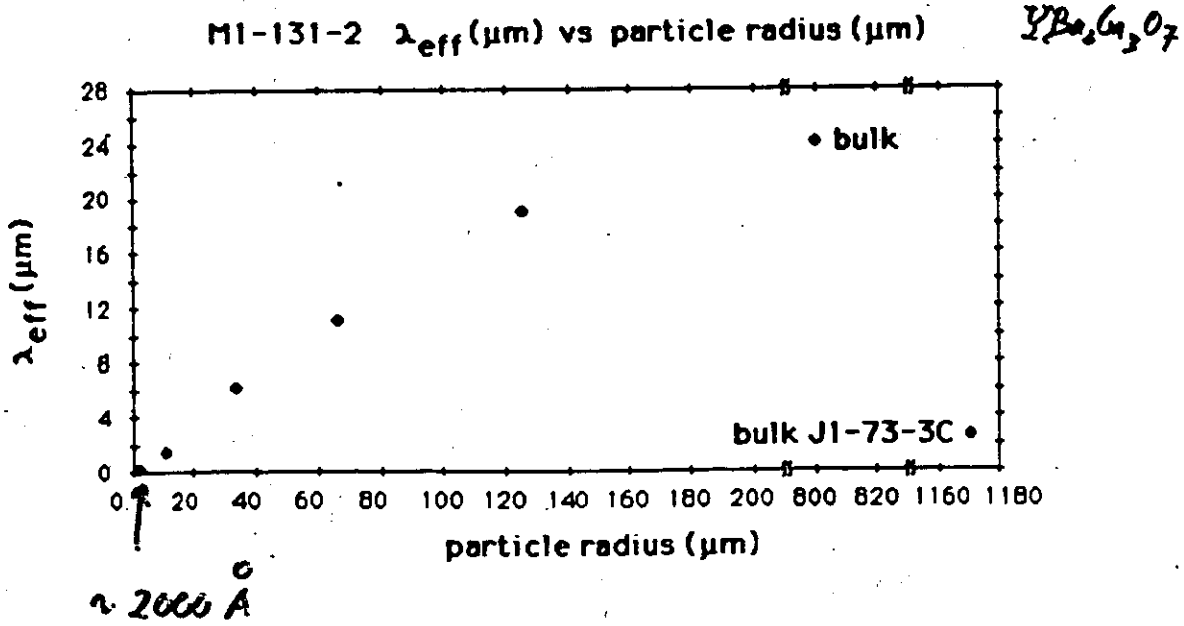

DISTRIBUTION OF FIELDS AND CURRENTS NEAR A JUNCTION

(de Gennes)

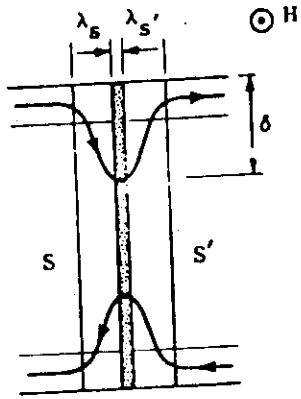

$$\delta^2 \cong \frac{\lambda \xi_0}{\pi}$$

Figure 7-5
Current streamlines around an S-N-S′ junction under a very weak applied field. Because of the weak current capacity of the junction, the field penetrates up to a large distance δ.

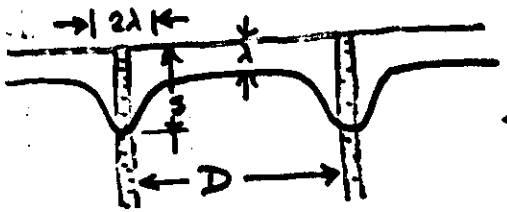

$$\langle \lambda^2 \rangle \cong \frac{s^2 \cdot 2\lambda + \lambda^2 D}{D + 2\lambda}$$

$$\langle \lambda^2 \rangle^{1/2} \simeq \lambda \left[\frac{\xi_0}{D\pi} \right]^{1/2}$$

ANOTHER MEASURABLE QUANTITY: MAGNETIZATION

$I \equiv$ magnetic dipole moment per unit volume, i.e., "induced magnetic intensity."

measurable $\Rightarrow$ $M \equiv \int_{\text{volume}} I\,dV =$ magnetic moment of sample, i.e., it's "magnetization," induced by an applied field H_a.

in the sample: $B = \mu_0 H_a^* + 4\pi I$

susceptibility: $I = \left(\frac{\mu_0}{4\pi}\right) \chi H_a$

- in Perfect Meissner state: $\chi = -1$
  i.e. infinite superconductor at very low field

* for no demagnetization factor (thin slab, cylinder & H_a)

in general: $B = \mu_0 H_i + 4\pi I$

$\mu_0 H_i = \mu_0 H_a - D I \cdot 4\pi$

D demagnetization factor

$$\kappa \equiv \frac{\lambda \leftarrow \text{magnetic penetration depth}}{\xi \leftarrow \text{coherence length}}$$

if $\kappa < \frac{1}{\sqrt{2}}$ positive surface energy ; type I

if $\kappa > \frac{1}{\sqrt{2}}$ negative surface energy; type II

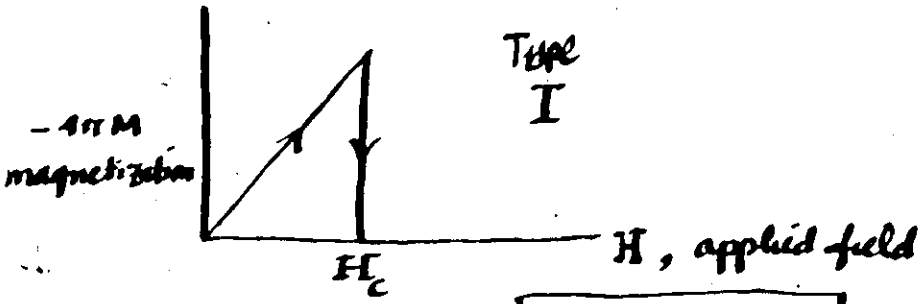

$$4\pi M + \mu_0 H = B$$

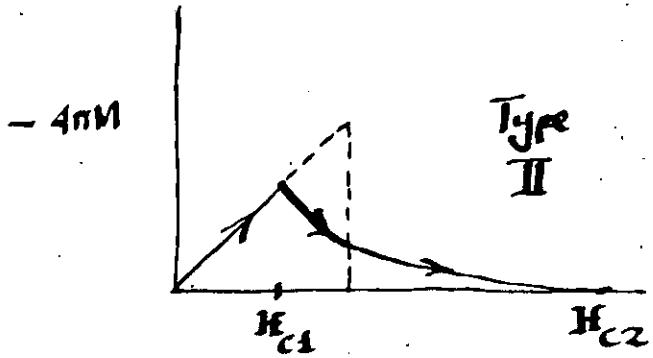

THERMODYNAMICS OF SUPERCONDUCTORS

- Work done to change volume of body by pressure:

$$dW_V = -p\,dV$$

- Work done to change magnetization of body by applied magnetic field:

$$dW_M = +\mu_0 H_a\,dM$$

- First law of thermodynamics:

$$dU = T\,dS - p\,dV + \mu_0 H_0\,dM$$

- Gibbs free energy:

$$G = U - TS + pV - \mu_0 H_0 M$$

- Change in Gibbs free energy due to magnetization:

$$G(H_a) - G(0) = -\mu_0 \int_0^{H_a} M\,dH_a$$

- Gibbs free energy density of superconducting material:

$$g_s(T,H) = g_s(T,0) - \mu_0 \int I \, dH_a$$

but $I = -H_a$ in superconducting region

$$\therefore \quad g_s(T,H) = g_s(T,0) + \frac{1}{2}\mu_0 H_a^2$$

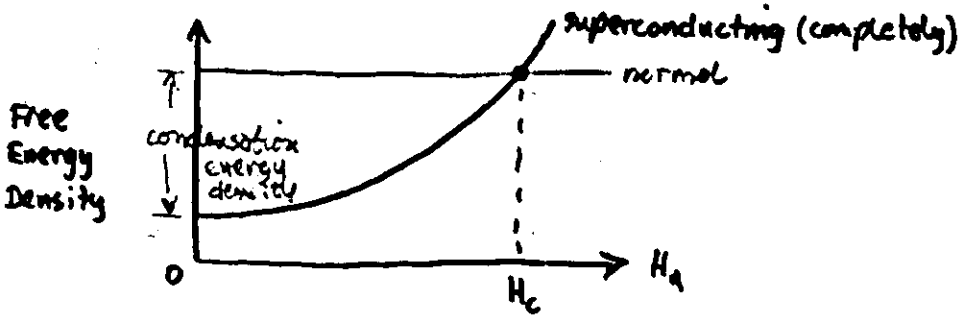

$\therefore$ for type I s.c.s $\Rightarrow$

$\therefore$ for both types I & II:

$$\text{condensation energy density} = -\frac{1}{2}\mu_c H_c^2$$

when $B_c = \mu_c H_c = 100$ gauss
cond energy dens. $= 398 \frac{\text{erg}}{\text{cm}^3}$

(or alternatively, $-\frac{B_c^2}{8\pi}$)

AT $H_a = H_c$

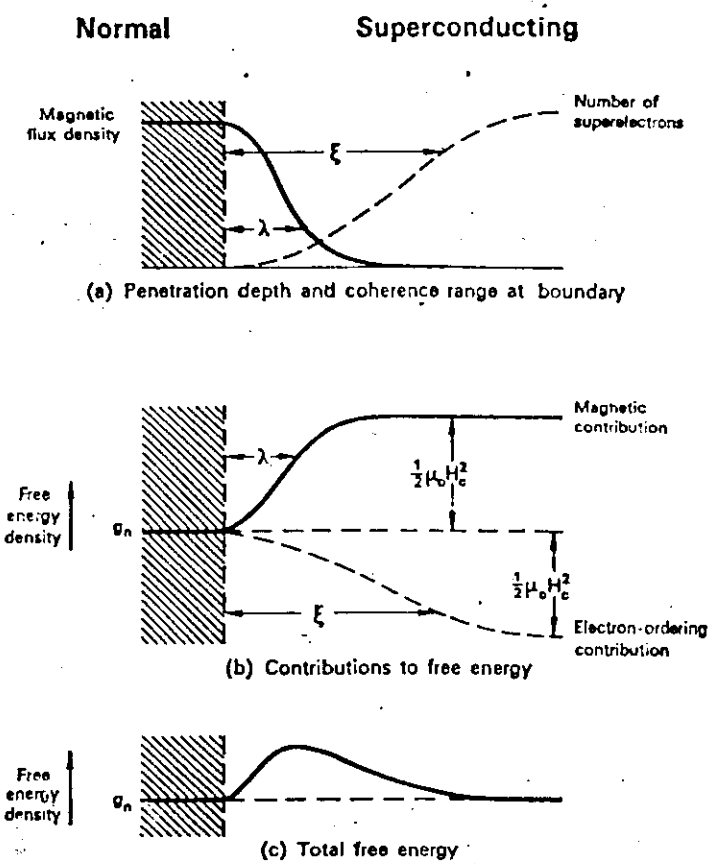

FIG. 6.8. Origin of positive surface energy.

It costs energy to make S/N boundary when $\frac{S}{\sqrt{2}} > \lambda$; HOMOGENEOUS S.C. STABLE : Type I

AT $H_a = H_c$

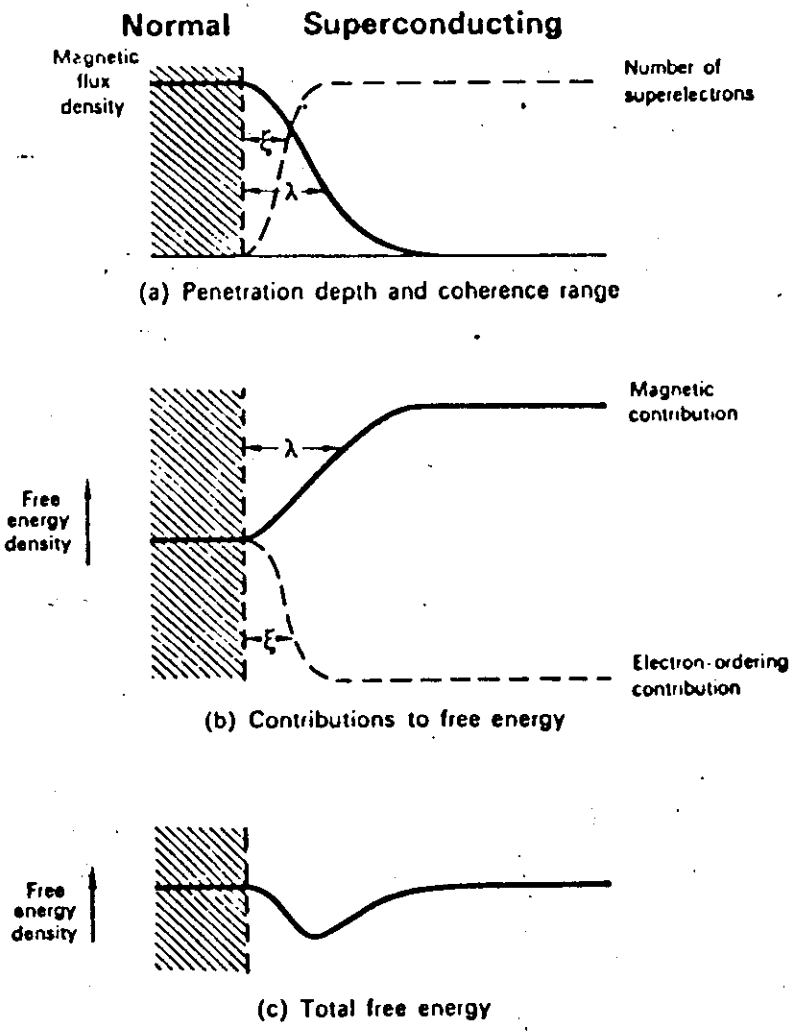

FIG. 12.1. Negative surface energy; coherence range less than penetration depth. (Compare this with Fig. 6.8.)

Energy is gained by making S/N boundaries if $\frac{\xi}{\sqrt{2}} < \lambda \Rightarrow$ INSTABILITY OF HOMOGENEOUS S.C. : Type II

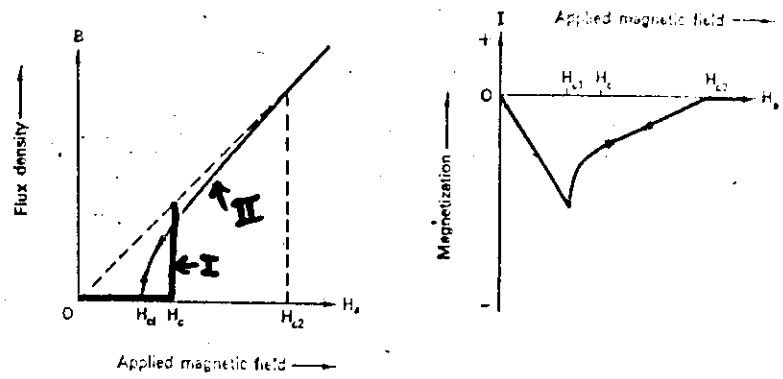

FIG. 12.7. Magnetization of a type-II superconductor.

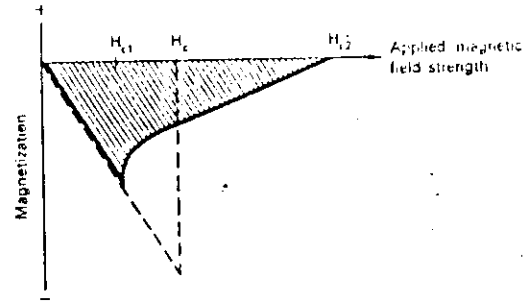

FIG. 12.8. Illustration of thermodynamic critical field H_c of type-II superconductor. The dotted right-angled triangle is drawn to have an area equal to the shaded area within the magnetization curve.

PHENOMENOLOGY OF THE MIXED STATE

• LONDON MODEL

Valid for $\kappa \gg 1$

$H_{c1} < H \ll H_{c2}$ when interaction between vortices is not too strong

above H_{c1}, homogeneous S.C. ⟶ vortices

vortex ≃ tube of normal phase embedded in superconducting phase

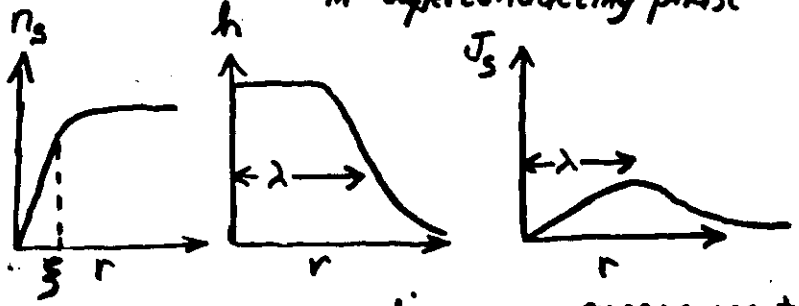

order parameter (s.c. electron density)

magnetic field

supercurrent density

→ $h(r) \approx \frac{\Phi_0}{2\pi\lambda^2}\left(\frac{\pi\lambda}{2r}\right)^{1/2} e^{-r/\lambda}$ for $r \gg \lambda$

energy per unit length: due to magnetic field, kinetic energy, core

→ $E_1 \simeq \frac{1}{2}\mu_0 H_c^2 \cdot 4\pi\xi^2 \ln(\lambda/\xi)$

London Model, cont.

• How Many Flux Quanta in a vortex?

$$E_1 = \int_{\text{outside core}} \left[\frac{h^2}{8\pi} + \frac{1}{2}mv_s^2 n_s\right] dS + \frac{1}{2}\mu_0 H_c^2 \pi\xi^2$$

$\frac{h^2}{8\pi}$: magnetic field energy; $\frac{1}{2}mv_s^2 n_s$: kinetic energy; $\frac{1}{2}\mu_0 H_c^2 \pi\xi^2$: core energy

$$\Downarrow$$

$$E_1 \simeq \left(\frac{n\Phi_0}{4\pi\lambda}\right)^2 \ln\left(\frac{\lambda}{\xi}\right) + \text{core energy}$$

$\therefore n = 1$ because $E_L(1) \neq 4E_L(1)$

$\Phi_0 = 2.07 \times 10^{-7}$ G-cm² (flux quantum)

• What is H_{c1}? (where Meissner state → mixed state)

minimize Gibbs free energy

$g = u - TS + pV - \mu_0 H_a I$ (neglect pV)

$u \sim NE_1$; $\mathcal{L} \sim -\frac{\mu_0 H_a B}{4\pi} + \frac{(\mu_0 H_a)^2}{4\pi}$

$N\Phi_0 = B$

$\therefore g \simeq B\left(\frac{E_1}{\Phi_0} - \frac{\mu_0 H_a}{4\pi}\right) + \frac{(\mu_0 H_a)^2}{4\pi}$

$$\Downarrow$$

$$\mu_0 H_{c1} = \frac{4\pi E_1}{\Phi_0} \simeq \frac{\Phi_0}{4\pi\lambda^2}\ln(\lambda/\xi)$$

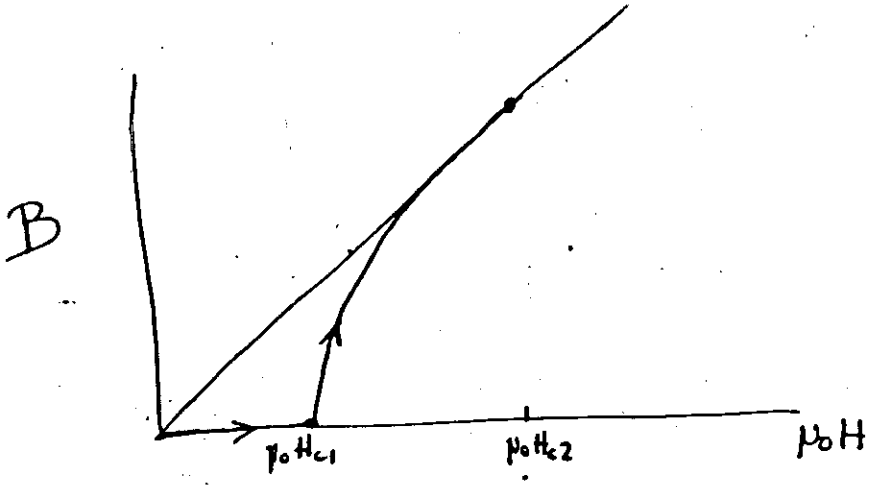

Near H_{c1} : (Fetter & Hohenberg)

$$B \simeq \frac{2\phi_0}{\sqrt{3}\lambda^2}\left\{\ln\left[\frac{3\phi_0}{\pi\lambda^2(H-H_{c1})}\right]\right\}^{-2}$$

↖ "Constitutive equation"

Vortex spacing:

$$\frac{d}{\lambda} = \left(\frac{2\phi_0}{\sqrt{3}\lambda^2 B}\right)^{1/2}$$

"2-fluid" approx.

$$\lambda(t) \simeq \frac{\lambda_0}{(1-t^4)^{1/2}}$$

$$H_{c1}(t) \simeq H_{c1}(0)\left(1-t^2\right)$$

where $t \equiv \frac{T}{T_c}$

For $YBa_2Cu_3O_7$:

$$\lambda_0 \simeq 1600\,\text{Å}$$

$$\mu_0 H_{c1}(0) \simeq 1500 \text{ gauss}$$

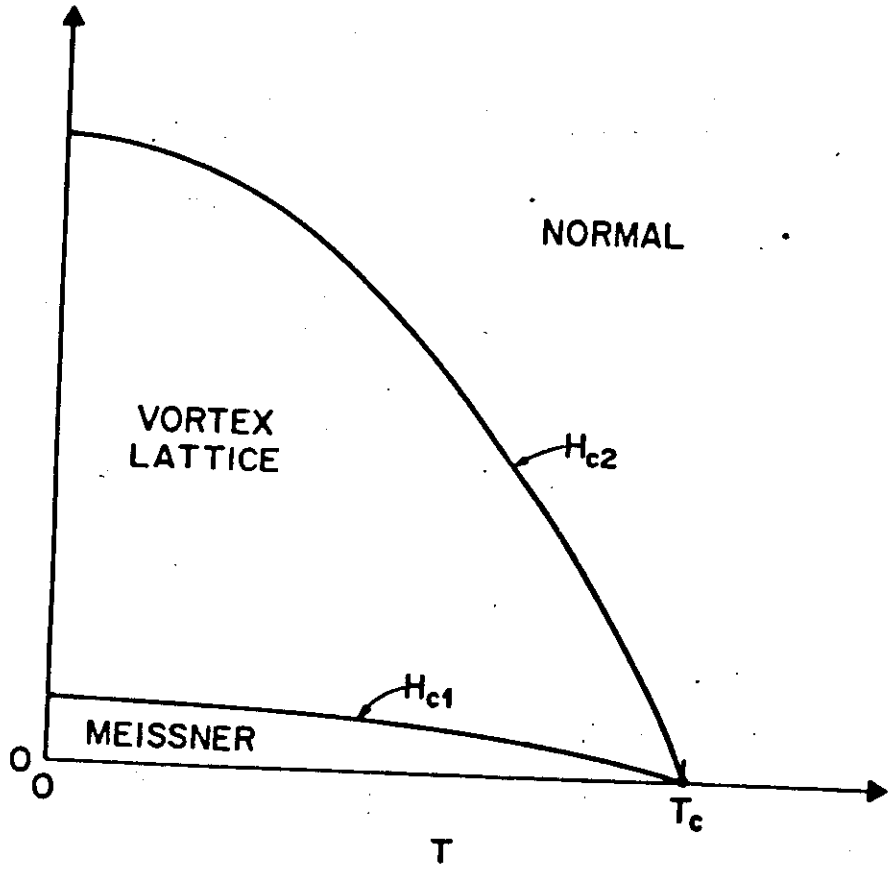

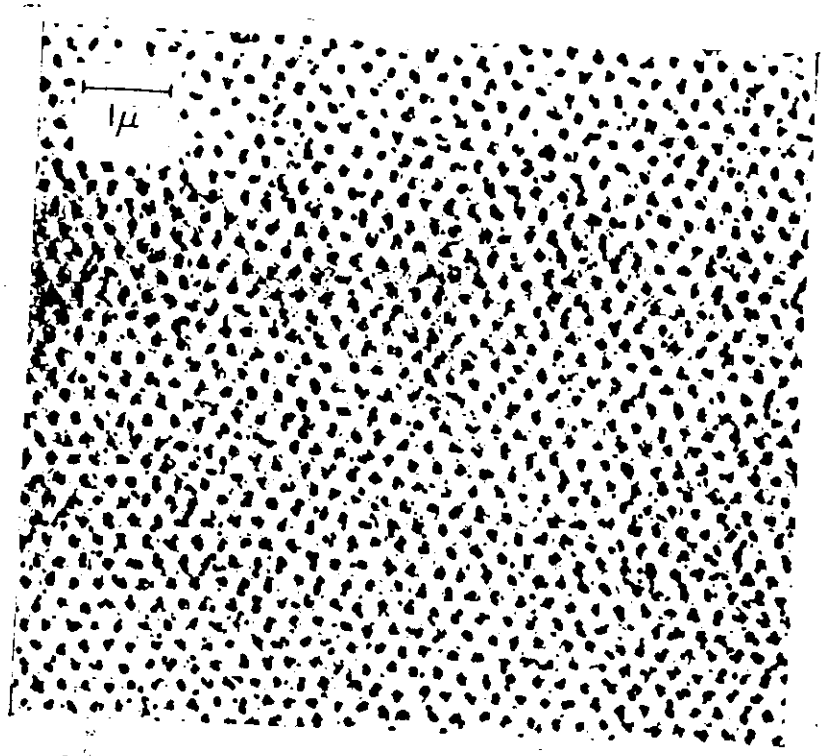

PATTERN OF INDIVIDUAL FLUXONS IN A TYPE-II SUPERCONDUCTOR
This photograph shows the triangular pattern of fluxons in a type-II superconductor (see Chapter 12). The pattern is revealed by allowing very small (500 Å) ferromagnetic particles to settle on the surface of a magnetized specimen (lead–indium alloy). The particles locate themselves where the magnetic flux intersects the surface. The photograph was obtained by electron microscopy of the deposited particles. (Photograph by courtesy of V. Essmann and H. Träuble, MAX PLANK Institut für Metallforschung.)

DEFECTS IN FLUX-LINE LATTICE

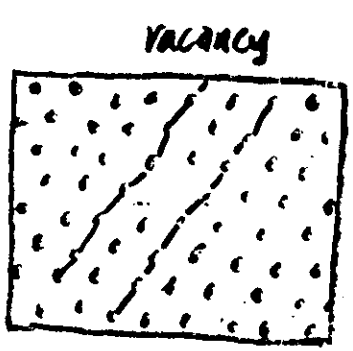

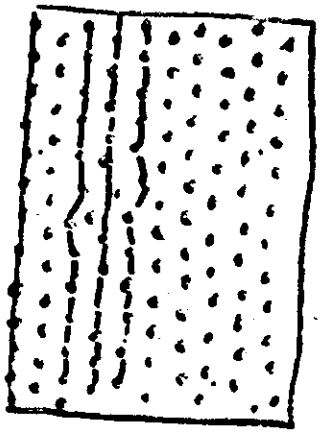

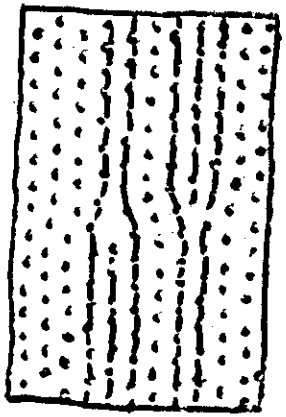

traced from photos of Träuble & Essmann in R. Huebner's book

H. Muller et al. (1990)

Anisotropic London Model (J. Clem, V. Kogan, ... L.J. Campbell, et al.)

Vortex centered on q_x-axis:

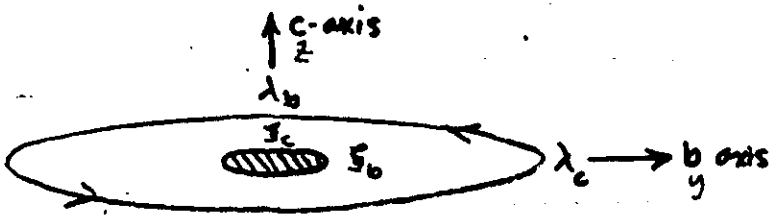

magnetic field outside core:

$$h_x(y,z) = \frac{\Phi_0}{2\pi\lambda_b\lambda_c} K_0(\zeta)$$

K_0 modified Bessel fn of order zero

$$K_0(\zeta) \simeq \left(\frac{\pi}{2\zeta}\right)^{1/2} e^{-\zeta} \quad \text{for } \zeta \gg 1$$

and

$$\zeta^2 \equiv \left(\frac{y}{\lambda_c}\right)^2 + \left(\frac{z}{\lambda_b}\right)^2$$

The c-axis component of H_{c1}:

(accounting only for magnetic field & kinetic energy densities)

$$H_{c1,a} \simeq \frac{\Phi_0}{4\pi\lambda_b\lambda_c} \ln\left(\frac{\lambda_b}{\xi_b}\right)$$

for $\frac{\lambda_c}{\xi_b} = \frac{\lambda_b}{\xi_a}$

and similar results by cyclic permutation $a \to b \to c \to a$, $x \to y \to z \to a$

Phenomenology of the Mixed State, Cont.

- Ginzburg - Landau Theory
- { London Theory is classical
  G.-L. theory uses quantum mechanics
  $|\Psi|^2$ = density of superconducting electrons }
- expansion of free-energy density:

$$f = f_n + \alpha|\Psi|^2 + \frac{\beta}{2}|\Psi|^4 + \frac{1}{2m^*}\left|\left(\frac{\hbar}{i}\nabla - \frac{e^*}{c}\vec{A}\right)\Psi\right|^2 + \frac{h^2}{8\pi}$$

- variational principle $\longrightarrow$ 2 G.-L. differential equations

Ψ, J_s, h .....

- Important Results (Isotropic case)
  - Abrikosov ordered vortex state near H_{c2}
  - elastic constants, ...
- $\mu_0 H_c = \frac{\Phi_0}{2\pi\sqrt{2}\,\xi\lambda}$ thermodynamic critical field
- $\mu_0 H_{c2} = \frac{\Phi_0}{2\pi\xi^2} = \sqrt{2}\,\kappa\, H_c$ upper critical field
- $\left.\frac{dI}{dH}\right|_{H_{c2}} = \frac{-1}{1.16(2\kappa^2-1)}$

• ANISOTROPIC EFFECTIVE MASS G-L. THEORY

(Klemm, Clem, Kogan .... Tilley)

Upper critical field:

$$H_{c2\,a} = \frac{\Phi_0}{2\pi \xi_b \xi_c}$$

and cyclic permutations $a \to b \to c \to a$

also solution for arbitrary angle of $\vec{H}$ relative to a, b, c

$$\tilde{\xi}_i = \frac{\xi}{\sqrt{m_i}} \quad \text{with} \quad m_a m_b m_c = 1$$

Thus: for $YBa_2Cu_3O_7$: $\xi_a : \xi_b : \xi_c = .8 : 1 : .2$

for $Bi_2Sr_2Ca_2Cu_3O_{10+\delta}$: $\xi_a : \xi_b : \xi_c \cong 1 : 1 : .02$

Thermodynamic critical field:

$$H_c = \frac{\Phi_0}{2\pi\sqrt{2}\,\lambda\xi} \quad \text{where} \quad \lambda = (\lambda_a\lambda_b\lambda_c)^{1/3}$$
$$\xi = (\xi_a \xi_b \xi_c)^{1/3}$$

• EXOTIC POSSIBILITIES, CONT.

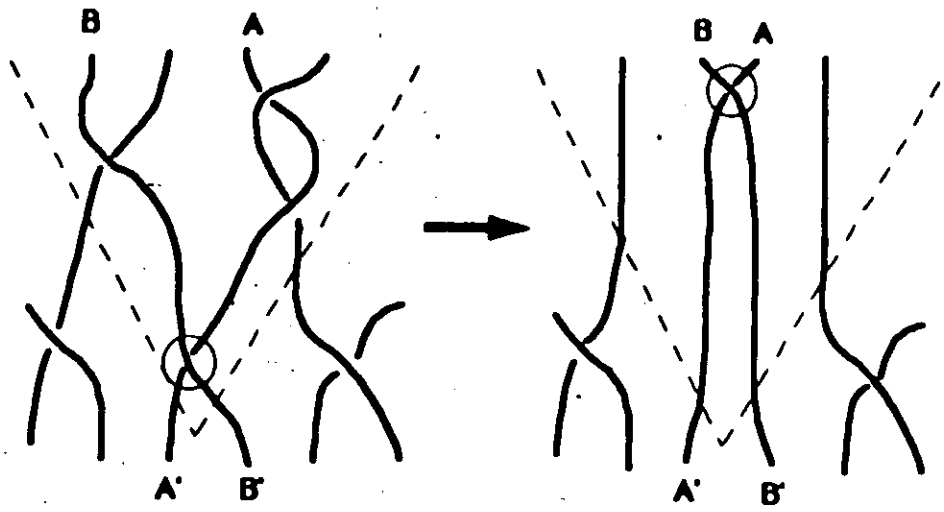

Fig. 3

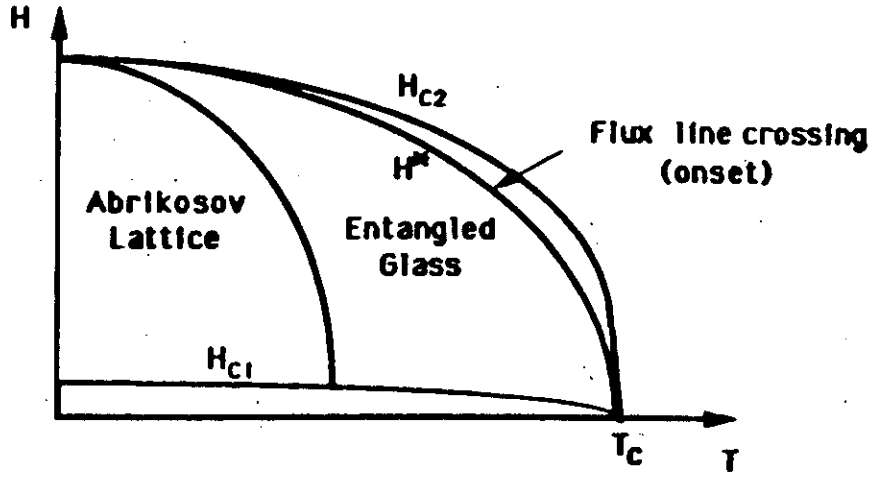

Fig. 4

(Obukhov & Rubinstein, 1991)

• OTHER EXOTIC POSSIBILITIES INCLUDE:

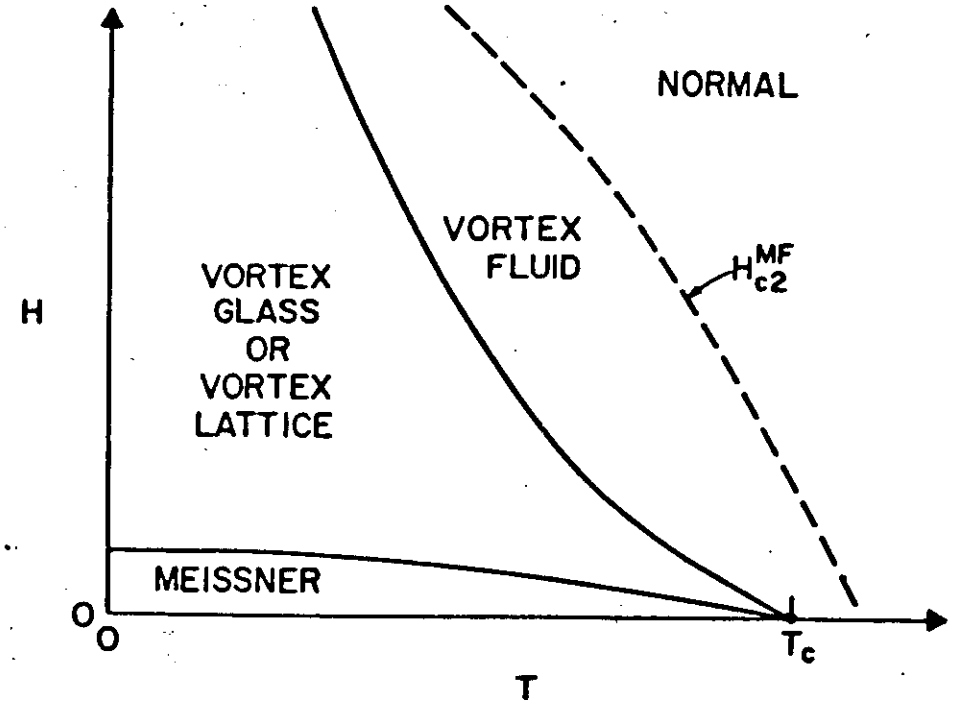

(Fisher, Fisher, & Huse, 1991)

Orlando et al
MIT

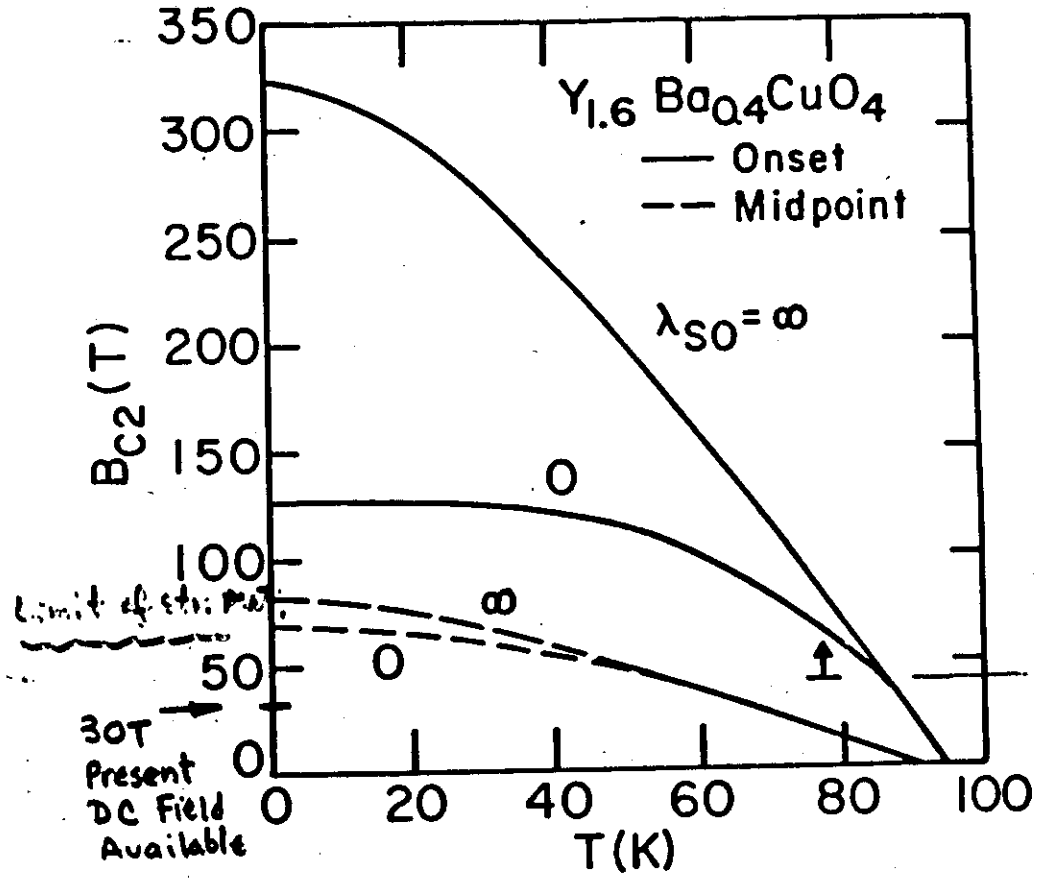

Figure 2

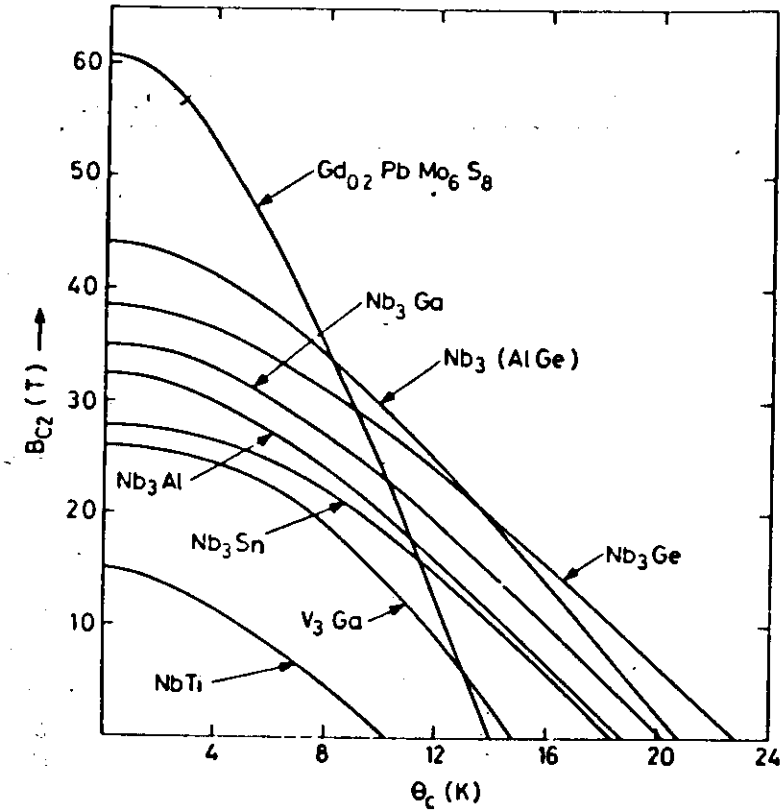

Fig. 12.16. Relationship between critical field and temperature of the best high-field superconductors.

TEMPERATURE DEPENDENCE OF λ, ξ

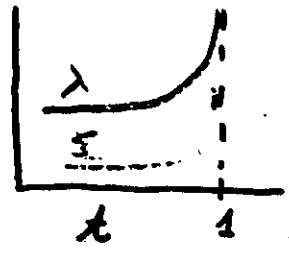

where $t = \frac{T}{T_c}$

- Empirically: $\lambda \simeq \frac{\lambda_0}{(1-t^4)^{1/2}}$ over wide range of t

- G.-L. Theory near T_c ($t \simeq 1$):

$$\lambda \simeq \frac{\lambda_0'}{\sqrt{2}(1-t)^{1/2}}$$

$$\xi \simeq \frac{\xi_0'}{(1-t)^{1/2}}$$

WHEN $\xi \simeq$ interatomic spacing, "continuum" theories such as anisotropic London, G.-L., etc. must break down. The discrete nature of the atomic structure must be explicitly included in that case.

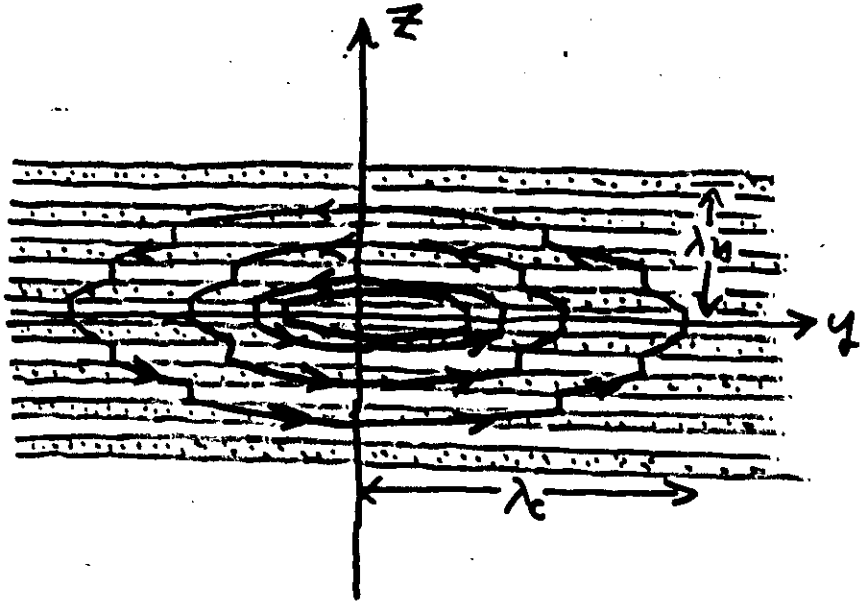

Josephson-coupled-layer model of vortex centered on x-axis [Clem & Coffey]

also similar model by Borone, Larkin & Ovchinnikov

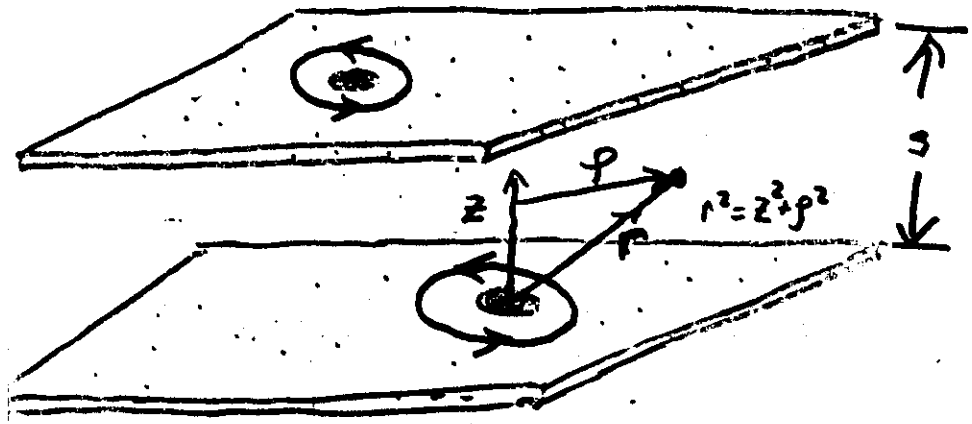

2-D vortex "pancake" model of Clem

[coupled-pancake model is a "formidable unsolved problem" J. Clem]

field & current distribution can be found:

e.g. $$h_\rho(r) = \frac{\Phi_0}{2\pi\Lambda} \cdot \frac{1}{\rho} \left\{ \frac{z}{|z|} e^{-\frac{|z|}{\lambda_\perp}} - \frac{z}{r} e^{-r/\lambda_\perp} \right\}$$

$$h_z(r) = \frac{\Phi_0}{2\pi\Lambda} \cdot \frac{1}{r} e^{-r/\lambda_\perp}$$

where $\Lambda = \lambda_\perp^2 / s$

can also get "inter-pancake" forces:

e.g. in same longer: long-range repulsive

$$F_\rho(\rho) = \left(\frac{\Phi_0}{2\pi}\right)^2 \frac{1}{\Lambda \rho}$$

C can lead to divergent rms displacements as $T \uparrow$

IRREVERSIBILITY

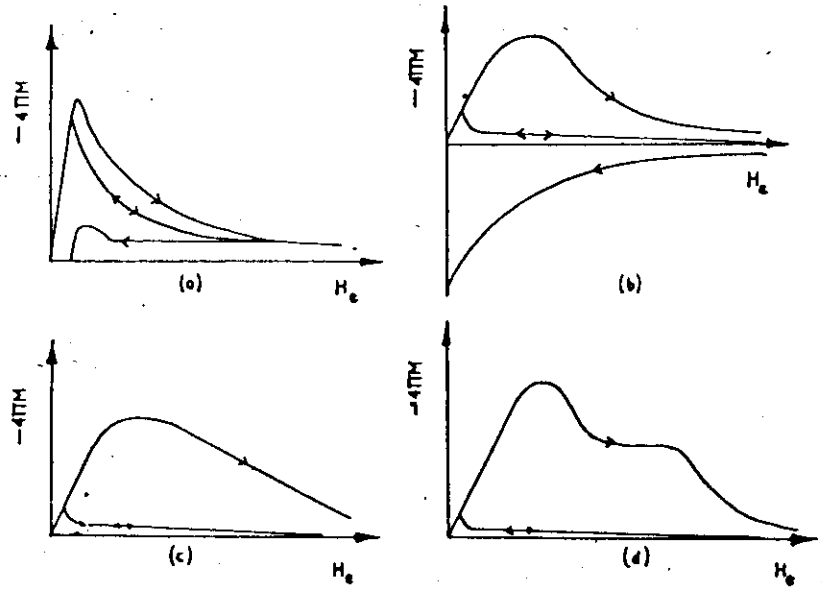

FIG. 8.7. Magnetization curves for four types of pinning centres calculated by Campbell *et al.* (1964): (a) for weak pinning; (b) for strong pinning; (c) closely spaced pinning centres; (d) a mixture of strong widely spaced centres and weak closely spaced centres

Also essential for consideration of charged particle motion is the Lorentz force equation,

$$\mathbf{F} = q\left(\mathbf{E} + \frac{\mathbf{v}}{c} \times \mathbf{B}\right) \tag{I.3}$$

that gives the force acting on a point charge q in the presence of electromagnetic fields.

Classical Electrodynamics

JOHN DAVID JACKSON

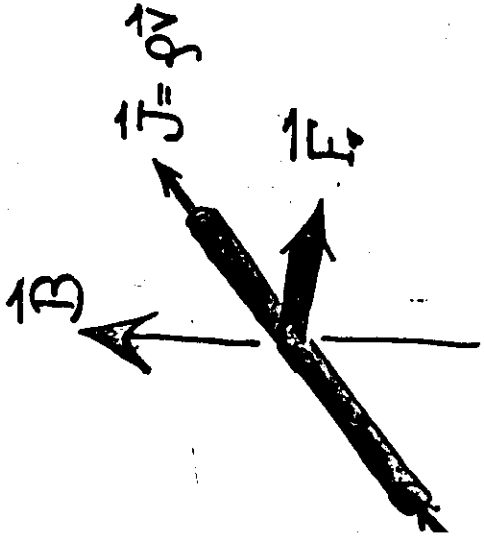

graphic evidence of flux pinning

Chip made of superconducting material, trapped in magnetic field, dangling below ... long as the chip stays cold ... enough, it will stay suspended.

C. Y. Huang, Lockheed Missiles and Space Co.

Suspension Effect Astounds Scientists*

Superconductors produce a mysterious new phenomenon.

By GEORGE JOHNSON

the phenomenon.

The effect came to light earlier this year in a classic case of scientific serendipity. Dr. Palmer N. Peters, a physicist at the National Aeronautics and Space Administration's Space Science Laboratory in Huntsville, Ala., was experimenting with a small ceramic disk that was cooled so that it acted as a superconducter.

Superconductors are materials

* only those scientists who never heard of flux pinning in type II superconductors!

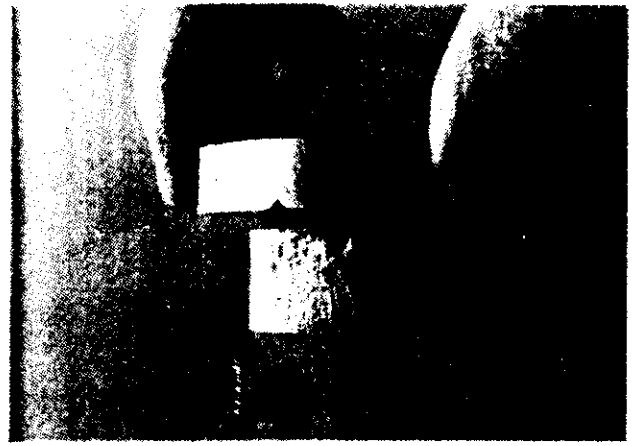

Murakami et al.
(ISTEC, Japan, 1989)

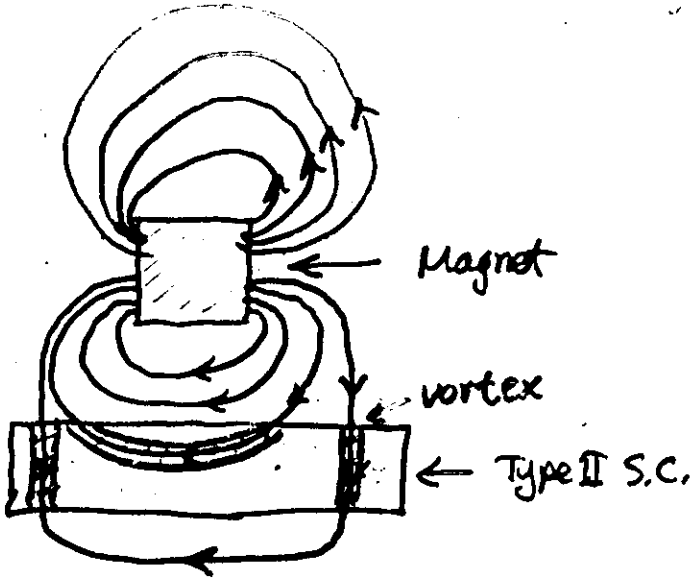

Remove Magnet

Hellman et al, J.A.P. 63, 447 ('88)
Brandt, A.P.L. 53, 1554 ('88)

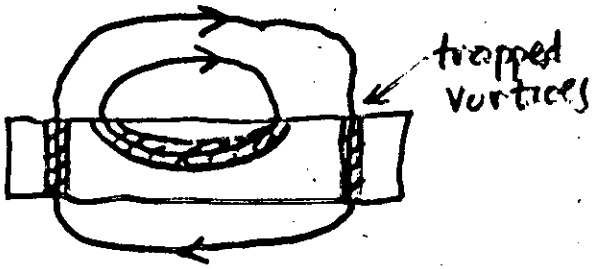

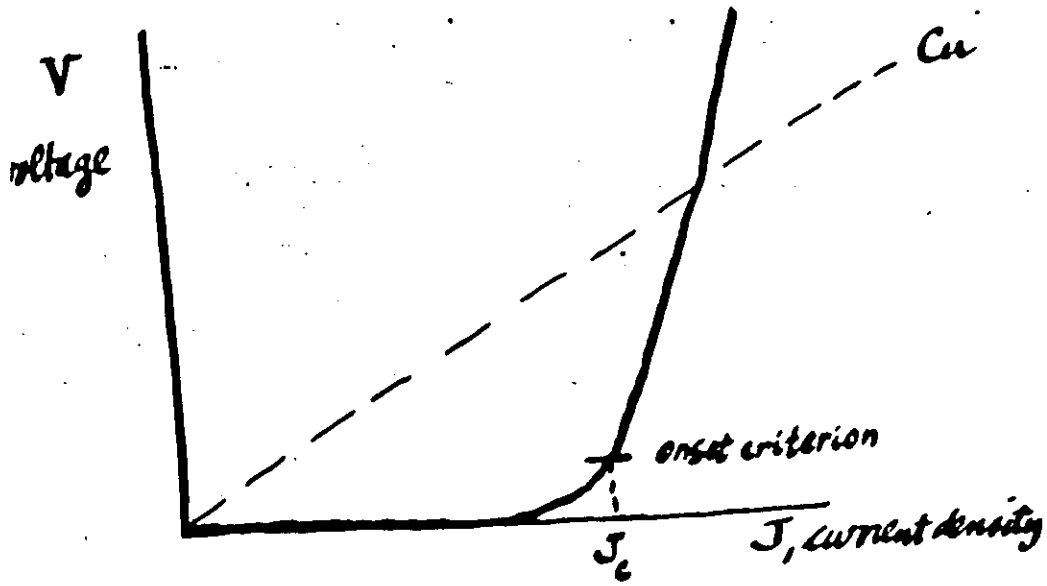

ρ_c (superconductor) $\simeq 10^{-12}$ Ωcm

ρ_{Cu} (77K) $\simeq 2 \times 10^{-7}$ Ωcm

Operational definition of critical current density

Upper Limit on J_c :

- Kinetic energy density ≈ condensation energy

⇓

depairing J_c

(See Tinkham p118)

$$J_c \simeq \frac{H_c}{\lambda_L} \propto \left(1 - \frac{T}{T_c}\right)^{3/2}$$

For $YBa_2Cu_3O_7$:

at 4.2K $J_c \simeq 2 \times 10^8 \, A\,cm^{-2}$

at 77K $J_c \simeq 2 \times 10^7 \, A\,cm^{-2}$

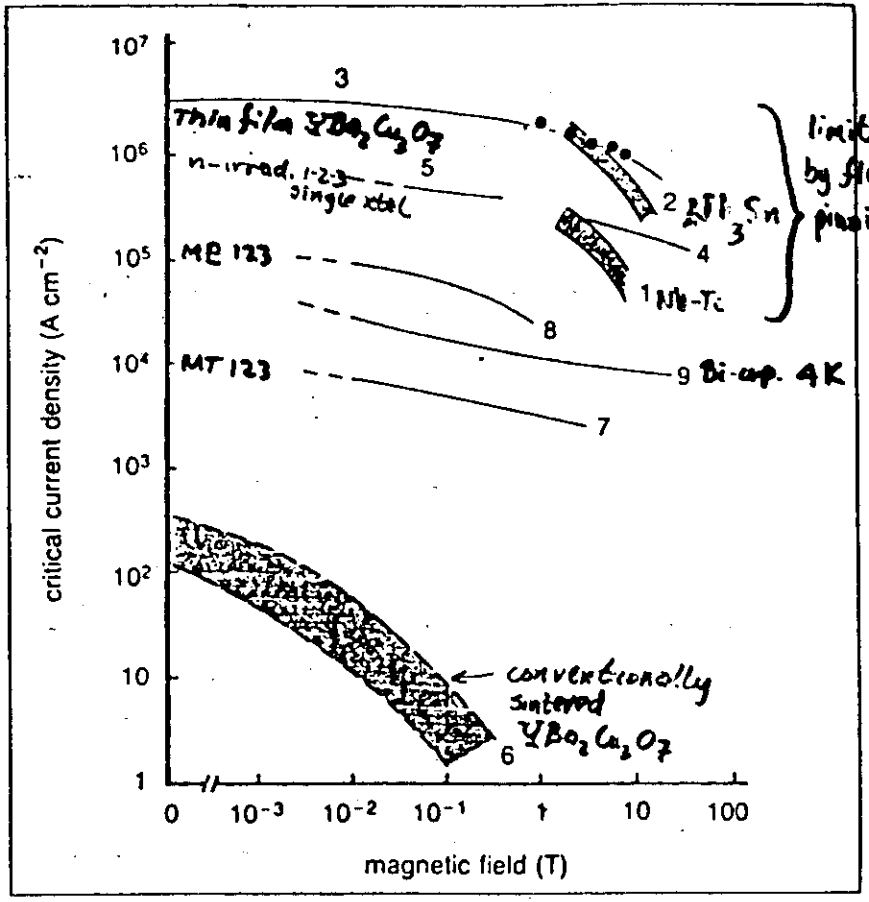

The variation of critical current density with magnetic field for different materials: 1 NbTi at 4 K; 2 Nb_3Sn at 4 K; 3 $Y_1Ba_2Cu_3O_7$ sputtered thin film at 77 K (Sumitomo); 4 $Y_1Ba_2Cu_3O_7$ MOCVD thin film at 77 K (Tohoku University); 5 $Y_1Ba_2Cu_3O_7$ neutron irradiated single crystal, critical current deduced from magnetisation at 77 K (AT&T Bell); 6 Typical values at 77 K for non-aligned polycrystalline $Y_1Ba_2Cu_3O_7$ bulk samples; 7 $Y_1Ba_2Cu_3O_7$ melt-textured wire at 77 K (AT&T Bell); 8 $Y_1Ba_2Cu_3O_7$ QMG processed sample at 77 K (Nippon Steel); 9 $Bi_2Sr_2Ca_1Cu_2O_{8+x}$ wire at 4 K (Vacuumschmelze)

J. Evetts, Phys. World ('90)

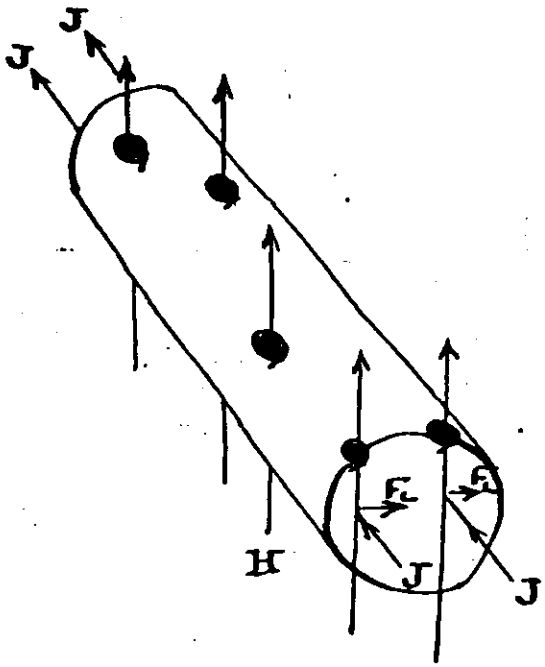

$F_L = J\varphi_0$

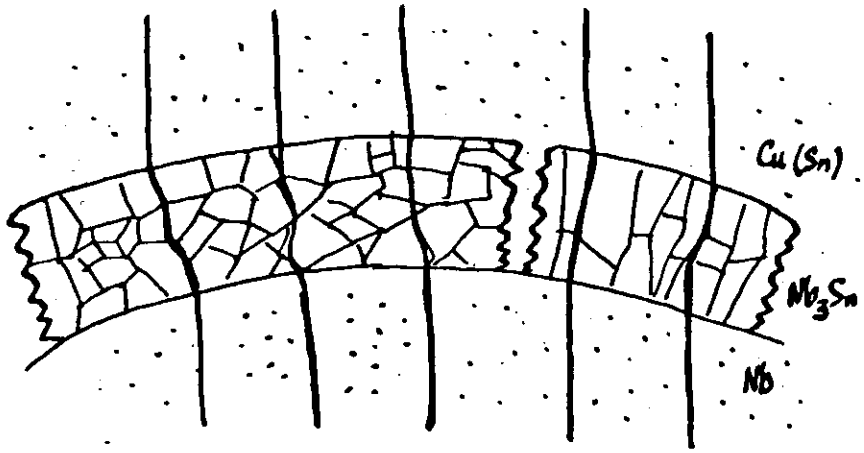

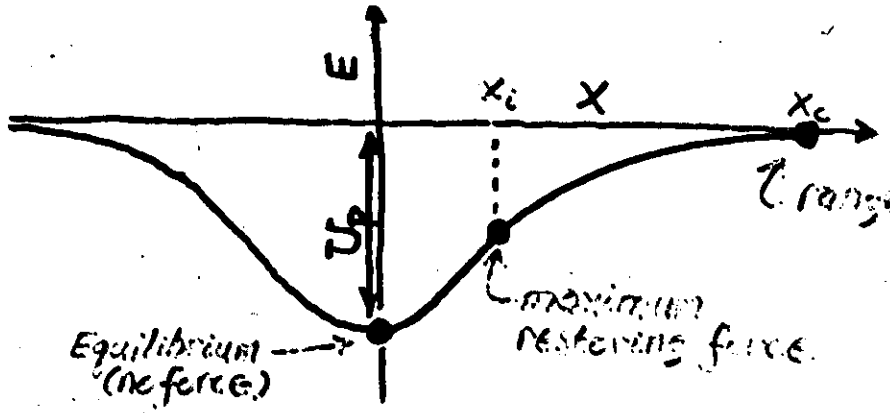

PINNING POTENTIAL ≡ E(x) as flux line(s) move with respect to defect

TWO ASPECTS :

- ENERGY → ACTIVATION ENERGY FOR FLUX CREEP U
- RESTORING FORCE → CRITICAL CURRENT DENSITY WITH NO THERMAL ACTIVATION $J_c(0)$

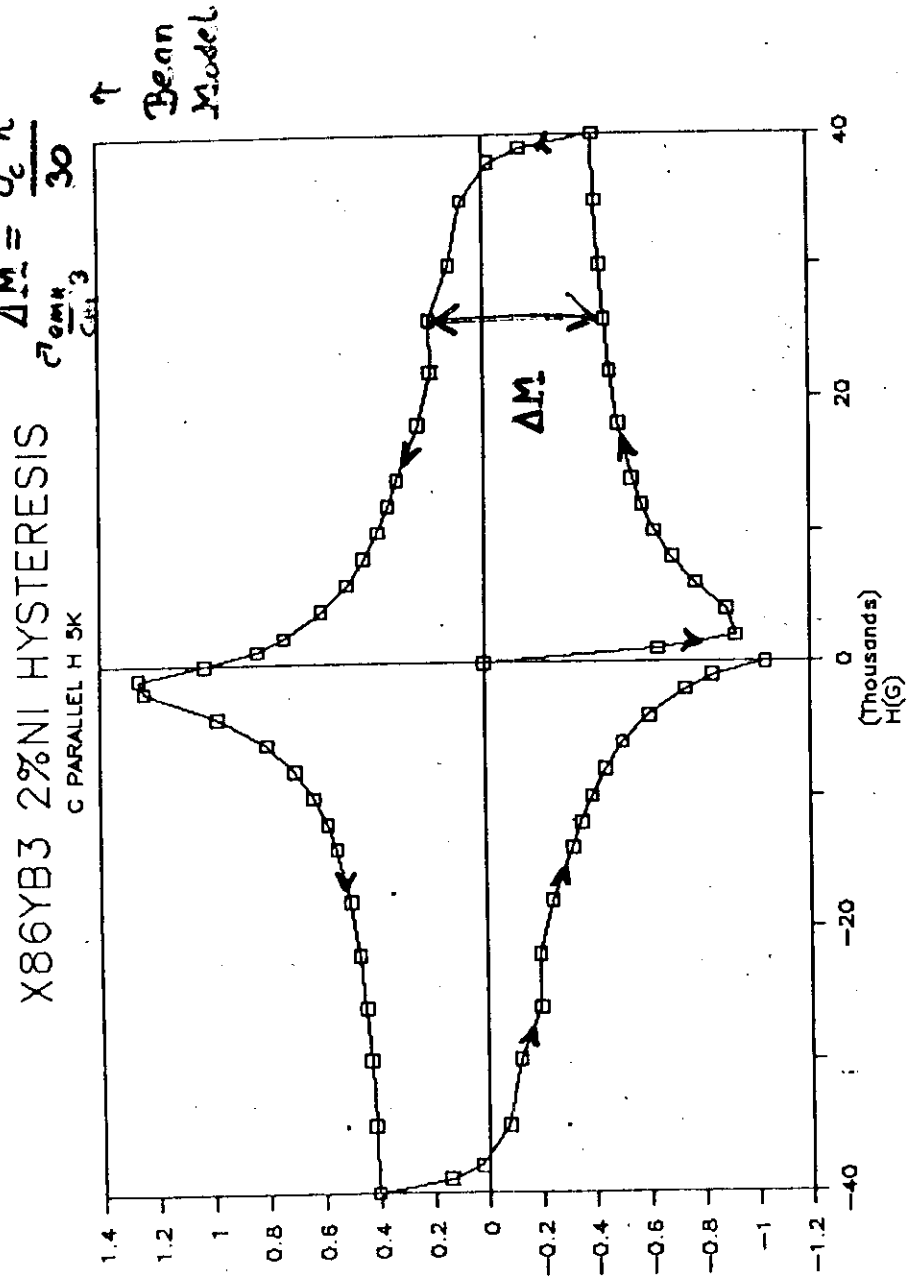

$$\Delta M = \frac{J_c R}{30}$$

↑ Bean Model

Suenaga et al.

$$\nabla \times \vec{B} = \mu_0 J_s$$

Critical State Approx^n:

$$J_s = J_c$$

CRITICAL STATE MODEL
(C. P. Bean)

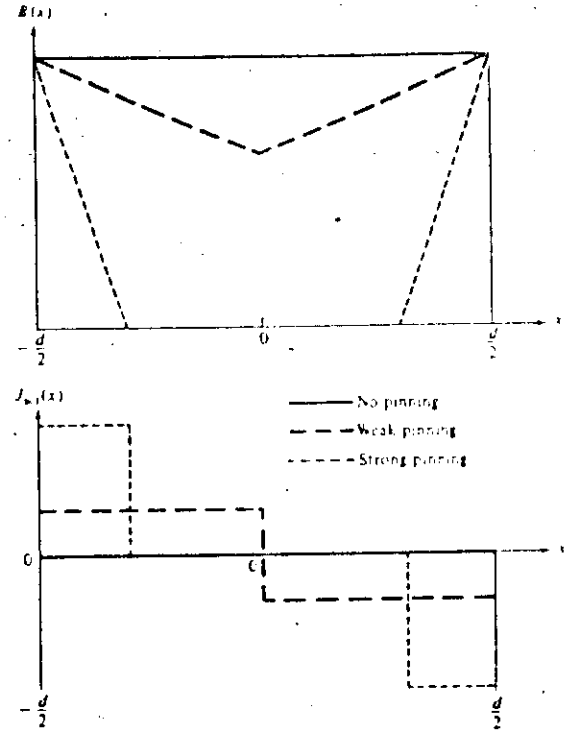

Figure 8.10a. Flux density and screening-current density for different pinning strengths according to the Bean critical-state model for a type II plate immersed in a parallel magnetic field, $H_{c1} < H < H_{c2}$.

Martin Wilson
Superconducting Magnets
p. 162

8.2. Hysteresis loss in the superconductor

8.2.1. *Slab parallel to the field*

We calculate the power generated G in a thin slab of thickness dx at a distance x from the penetration depth, using $G = J_c E = J_c d\phi/dt$ where ϕ is the change in flux enclosed. The loss per unit volume per half cycle may thus be found by integrating $J\,\Delta\phi(x)$ over the slab and dividing by the volume. From symmetry we need consider only half the slab

$$q = \frac{1}{a}\int_0^p J_c\,\Delta\phi(x)\,dx = \frac{1}{a}\int_0^p J_c\mu_0 J_c x^2\,dx = \mu_0 J_c^2 p^3/3a \qquad (8.5)$$

Hysteresis :

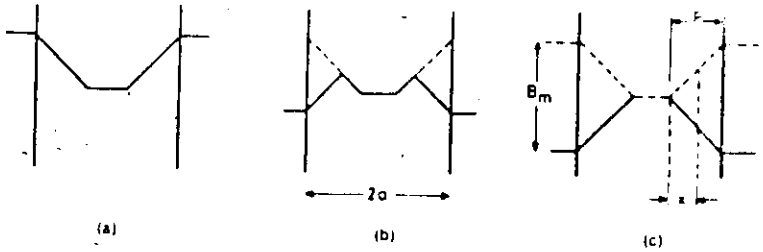

Fig 8.3. (a) Field pattern within a superconducting slab subjected to a small field change, (b) as the external field is reduced, (c) when the external field reaches minimum value before rising again.

where p is the penetration depth $= B_m/2\mu_0 J_c$ (remembering the conditioning effect of a previous field change in the opposite direction). It will be convenient for many of these calculations to define an amplitude of field oscillation B_p which just penetrates to the centre of the sample and to work in terms of the ratio $\beta = B_m/B_p$; in this case we have $B_p = 2\mu_0 J_c a$, i.e.

$$\beta = B_m/B_p = B_m/2\mu_0 J_c a. \qquad (8.6)$$

Substituting into eqn (8.5) and doubling to obtain the loss per cycle, we have

$$Q = \frac{B_m^2}{2\mu_0}\cdot\frac{\beta}{3} = \frac{B_m^2}{2\mu_0}\cdot\Gamma(\beta) \quad \text{for} \quad \beta < 1. \qquad (8.7)$$

We may loosely think of the first part of eqn (8.7) as being the energy available in the magnetic field oscillation and the second as the fraction of this energy which is actually dissipated.

Beam model works for $YBa_2Cu_3O_7$ thin films

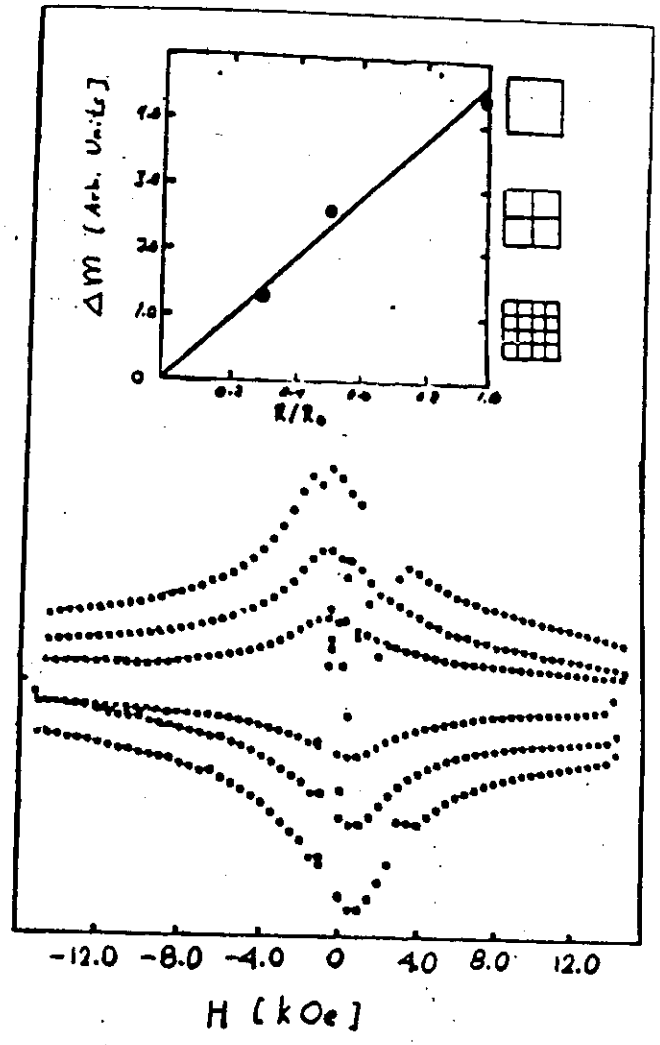

B. Oh et al.
Appl. Phys. Lett. 51, 852 (1987)

Fig 3.

Improved flux pinning caused by adding silicide precipitates

S. Whang et al. Polytechnic University

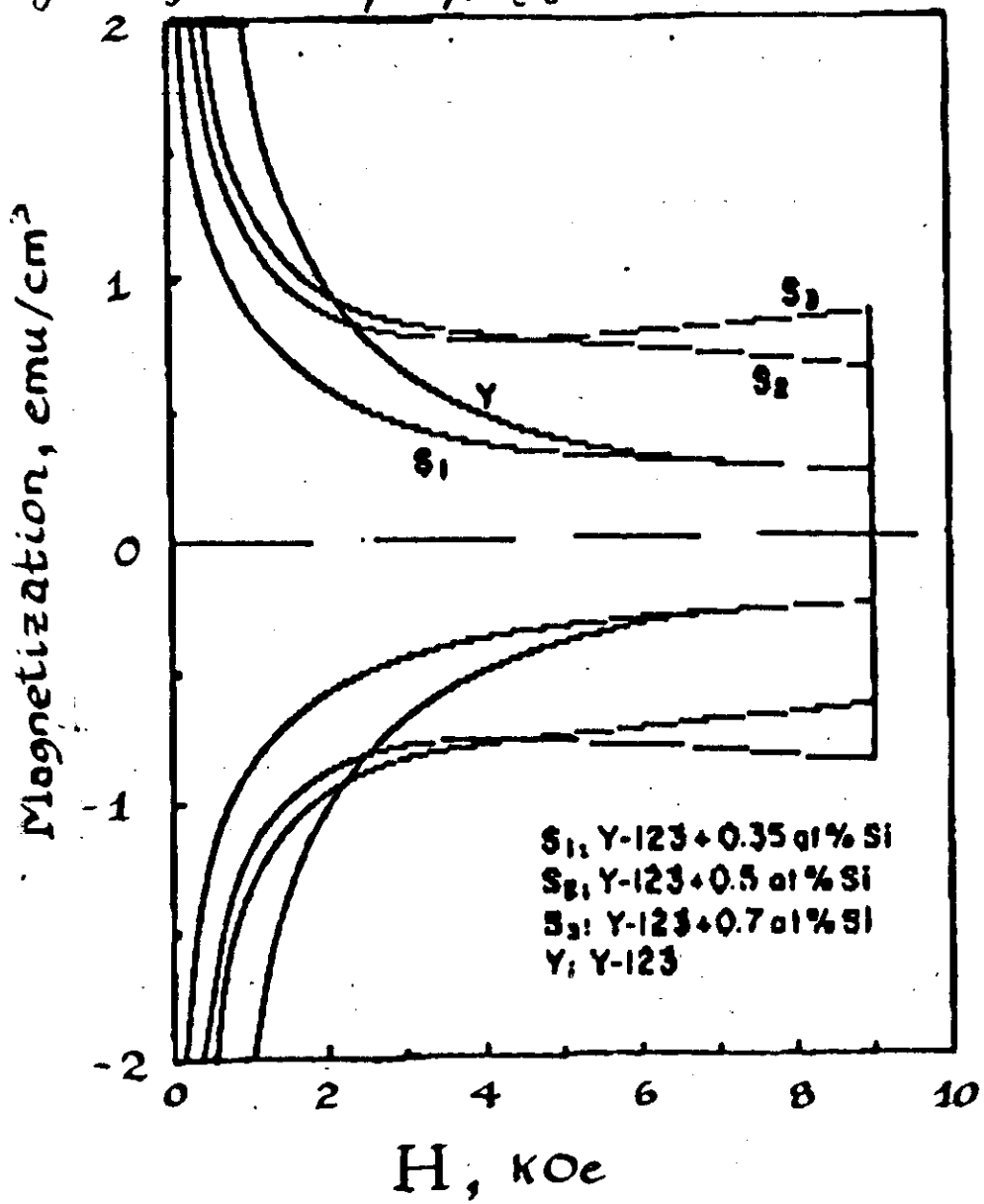

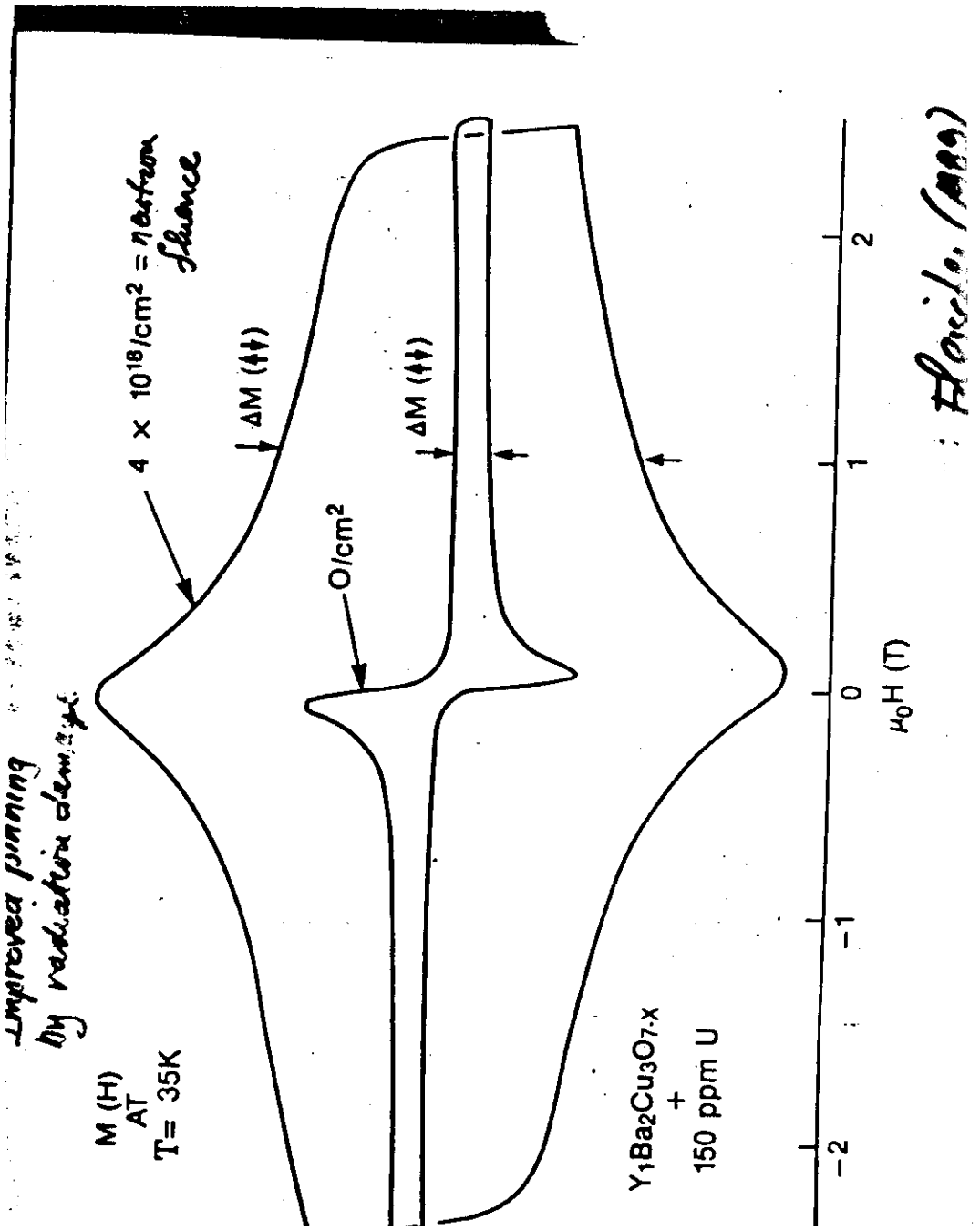

Improved pinning by radiation damage

Florio, (1989)

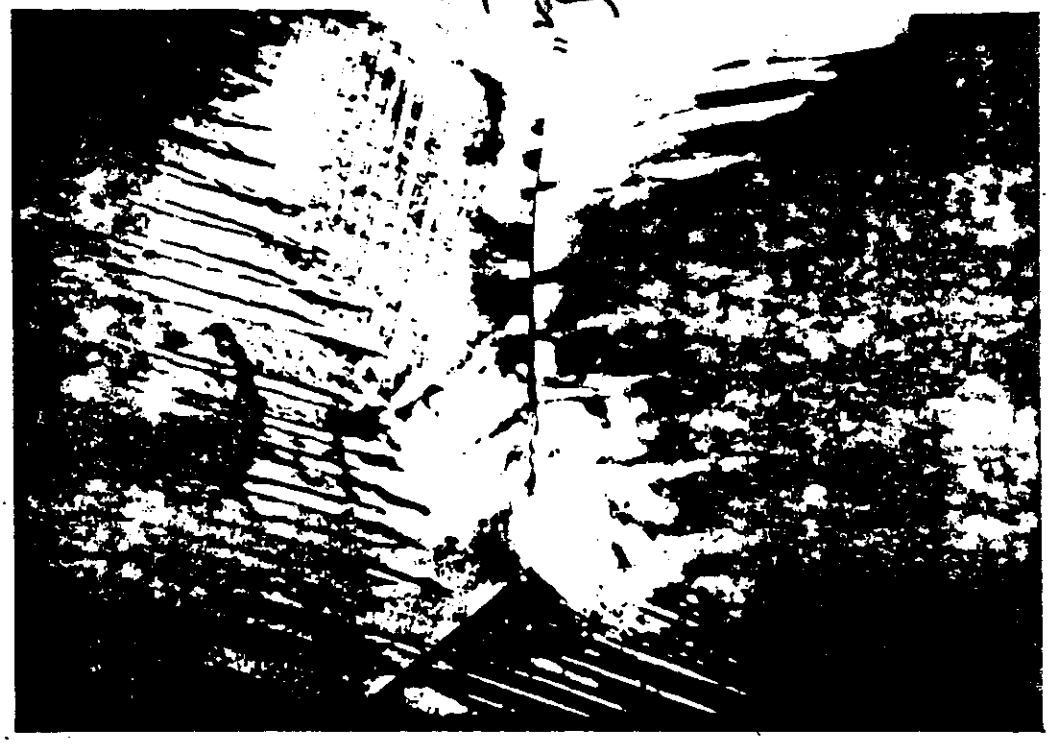

Hysteresis from intergranular material in $YBa_2Cu_3O_7$

Conclude: intergranular material acts like type-II Supercond.

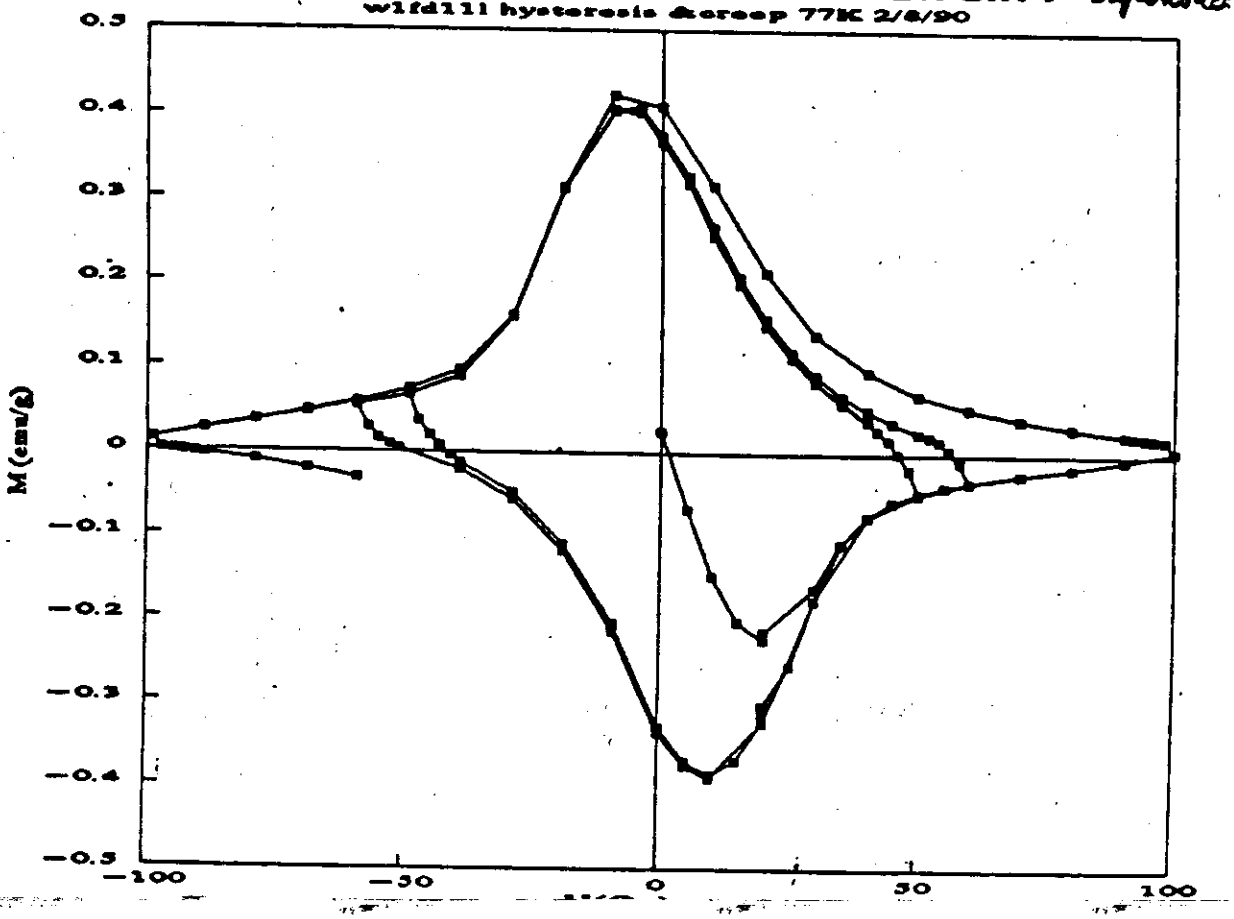

Major Issues in Flux Pinning

- What are the pinning centers?
- What is the mechanism of pinning?

pinning potential
pinning force

- "Summation Problem":

  Lorentz force on vortices
  Vortex-vortex interactions } complex many-body problem
  Vortex-pin interactions }

- In oxides: thermally activated depinning

"Solutions" to the Summation Problem

$$F_p \equiv \vec{J} \times \vec{B}$$

- Rigid FLL, random point pins

$$F_p = 0$$

- Collective Pinning Theory
  (Larkin & Ovchinnikov; Brandt; Ikeda, ...)

$$F_p = \left\{ \frac{n_v \langle f_p^2 \rangle}{V_c} \right\}^{1/2} = \left[\frac{1/2\, n_v f_p^2}{R_c^2 L_c} \right]^{1/2} \propto n_v^{1/2} f_p$$

V_c: correlation vol.

- Direct Summation

$$F_p = n_v f_p$$

- FLL Shear [Kramer; Brandt & Das]

$$F_p = \frac{2\tau_{max}}{w} = \frac{2A c_{66}}{w}$$

- **PINNING CENTERS**

  point defects & clusters

  dislocations and networks

  precipitates, voids

  stoichiometry and structure fluctuations

  grain boundaries, twin boundaries, stacking faults

  microcracks

  ⋮

- **PINNING MECHANISMS**

  variation of superconducting parameters
  $N(0), V, E_F \cdots$ "δT_c-pinning"

  quasiparticle scattering

  anisotropy of B_{c2}

  magnetic interactions

  elastic interaction

Flux Pinning

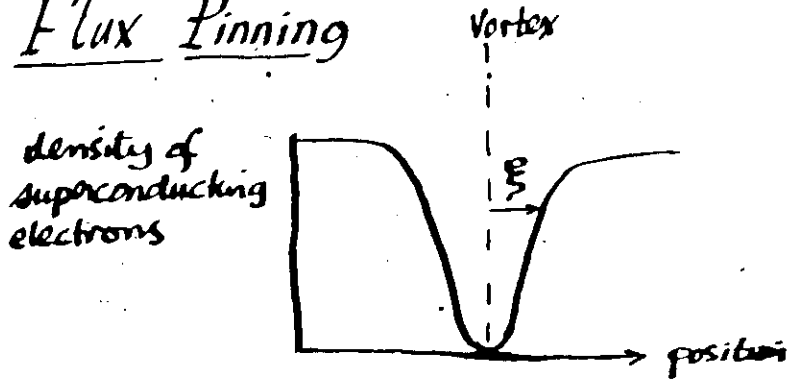

Condensation energy density $= \frac{1}{2}\mu_0 H_c^2$

$\therefore$ $\frac{\text{vortex core energy}}{\text{unit length}} \simeq \frac{1}{2}\mu_0 H_c^2 \cdot \pi\xi^2$

* Thus it is energetically favorable to put the flux lines in defective regions of crystal. ("size" $\gtrsim \xi$)

Binding Energy $= \frac{1}{2}\mu_0 H_c^2 \cdot \pi\xi^2 \cdot f$ (less than unity)

Watching Flux Creep:

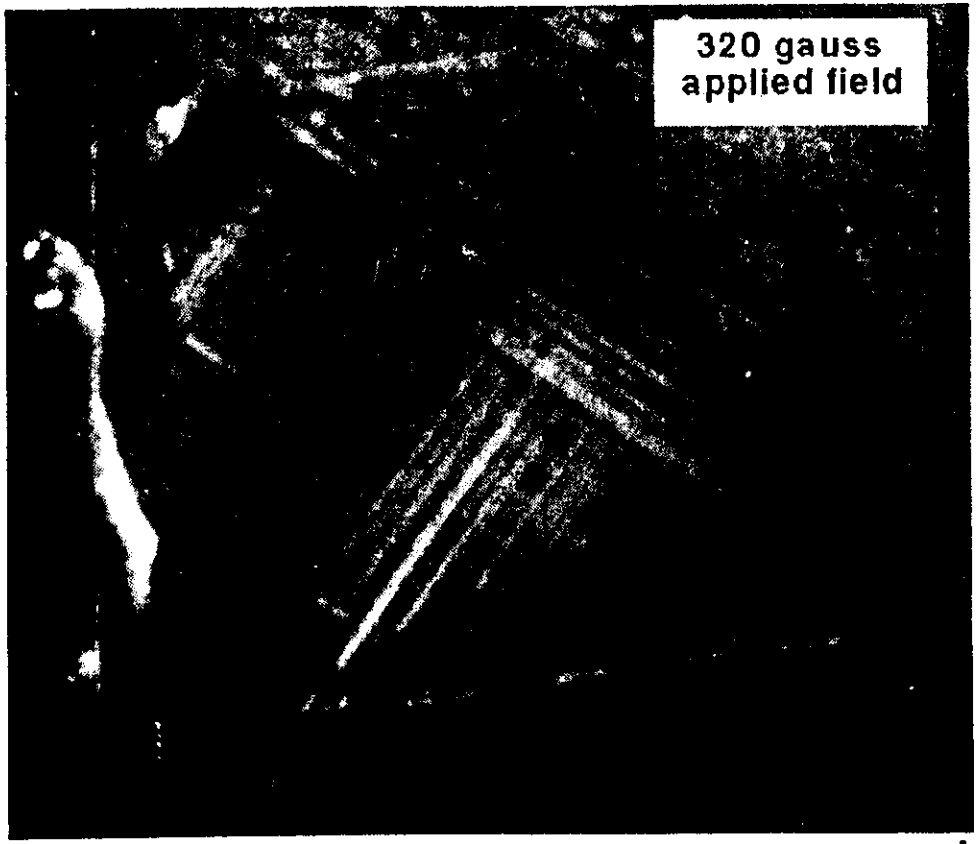

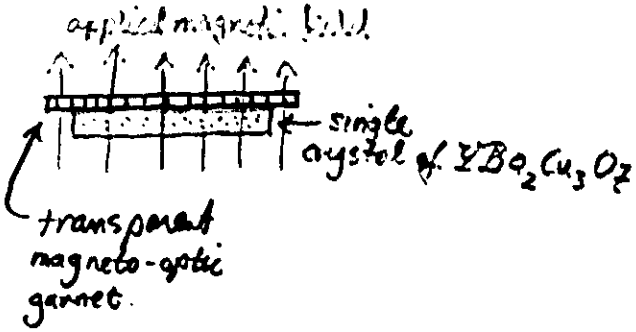

in polarized light:
2 domains visible for H_c Ha $\lesssim$ 150 gauss
and 1 domain for H_c Ha $\gtrsim$ 150 gauss
(case above)

H. Muller (1991)

Watching Flux Creep, cont.

- 4096 s
- 2048 s
- 1024 s
- 512 s
- 256 s
- 128 s

H_c Ha → 0 at t=0

—— 150 gauss contour at 128 s
..... 150 gauss contour at 4096 s

time dependence ~ ln t

H. Muller

Fluctuations and "Giant Flux Creep"

$$\frac{U_0}{kT} \simeq \frac{\frac{1}{2}\mu_0 H_c^2 \cdot \pi\xi^2 \cdot \ell}{kT}$$

probability of thermal depinning

$$\simeq \nu e^{-U/kT} \qquad U = U_0 f_n\left(\frac{J}{J_c}\right)$$

"low temp." superconductors: $U_0 \sim eV$

"high-temp." oxides : $U_0 \sim 0.01 - 0.1\ eV$

∴ flux creep can be a problem

Bi-oxides
Tl-oxides
Y-Ba-Cu-O

Quantitative measurement of Flux Creep

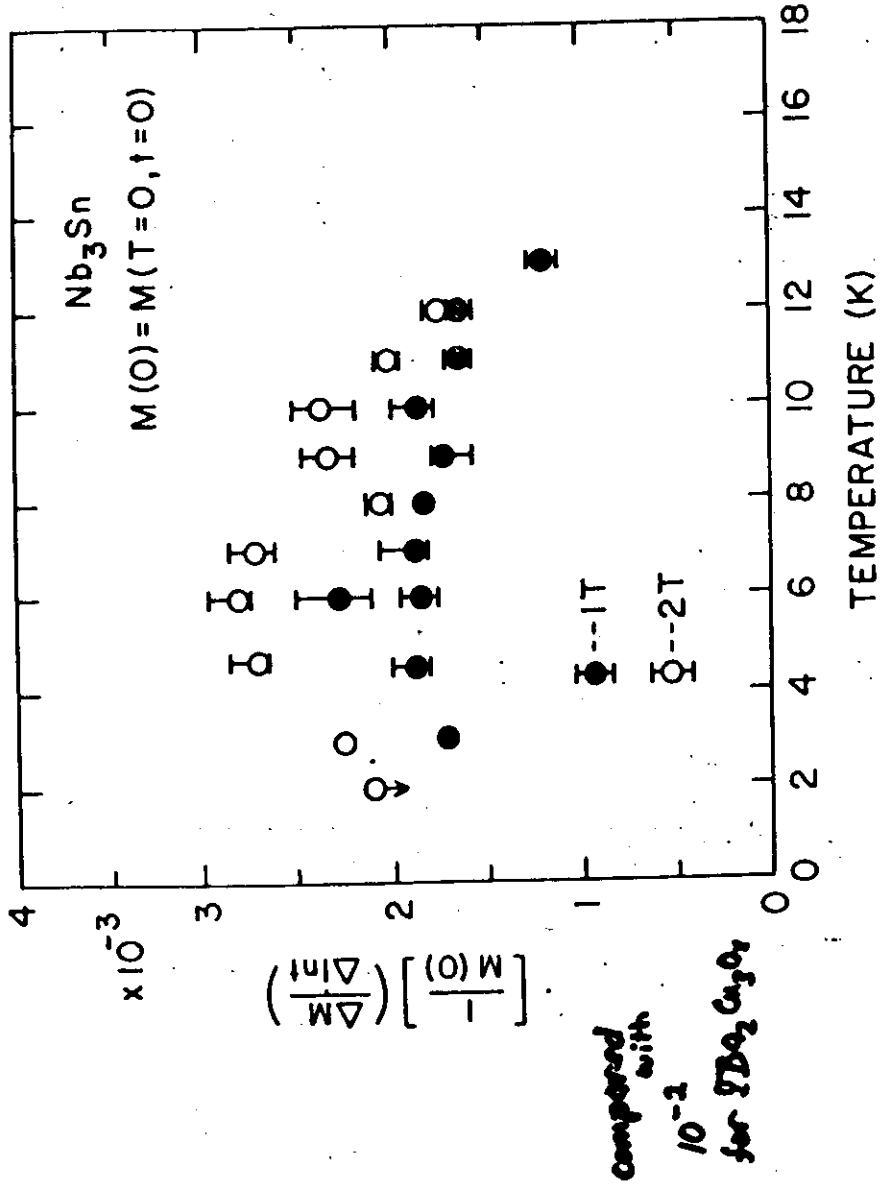

EXPECTED TEMPERATURE DEPENDENCE OF THE PINNING POTENTIAL

$$U_p \propto a_0^n \xi^m H_c^2 = f(T,B)$$

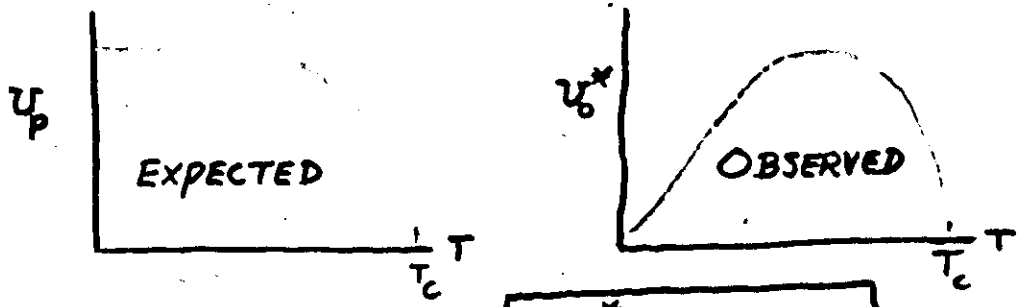

"CLASSICAL APPROACH" → Assume $U = U_p(1 - \frac{T}{T_c})$

$$U_0^* = \frac{-KT}{\frac{1}{M}\frac{dM}{dt}}$$

CONTRIBUTING FACTORS TO DISCREPANCY:

- Spectrum of Pinning Potentials

  Griessen et al. ('89)
  Gurevich et al. ('90)

- Non-Linearity of U vs. ∇B

  Beasley et al. ('69)

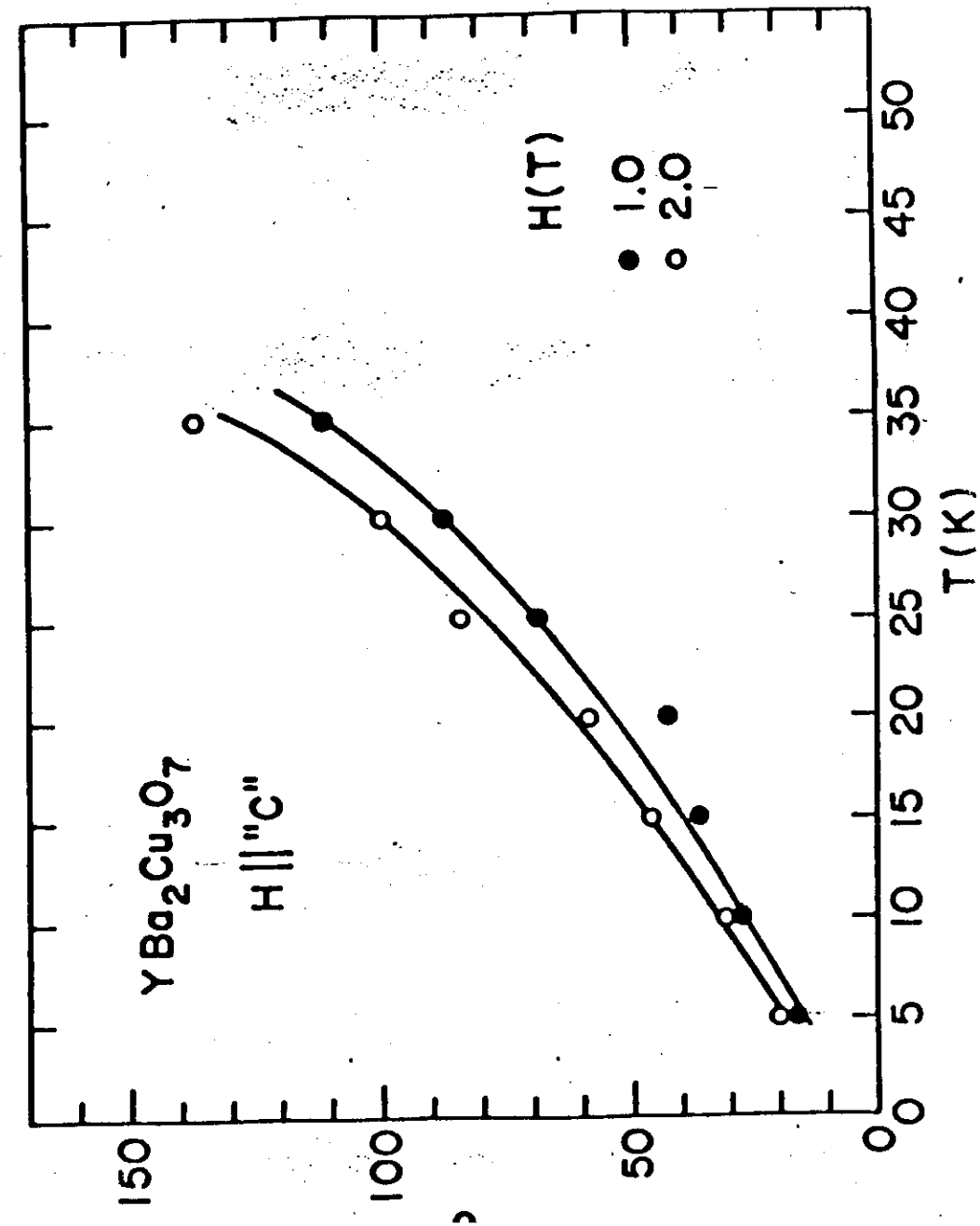

$$E(x) = -Fx + \frac{(x/x_0)^{20}}{1+(x/x_0)^{20}}$$

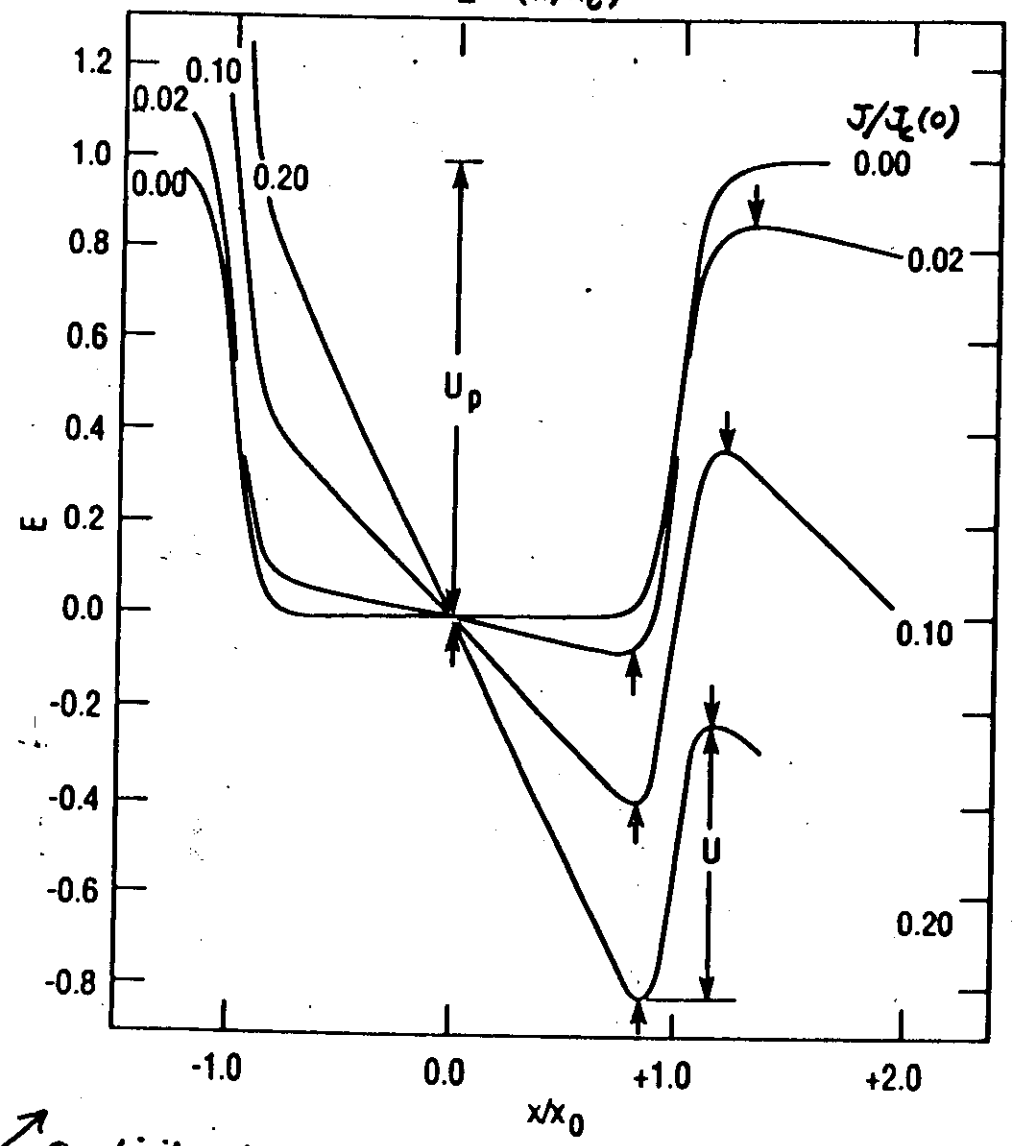

↖ Explicit calculation of depence of U on J/J_c

CONCLUSION: $U \approx U_p \left(1 - \frac{J}{J_c}\right)^n$ with $n \neq 1$!

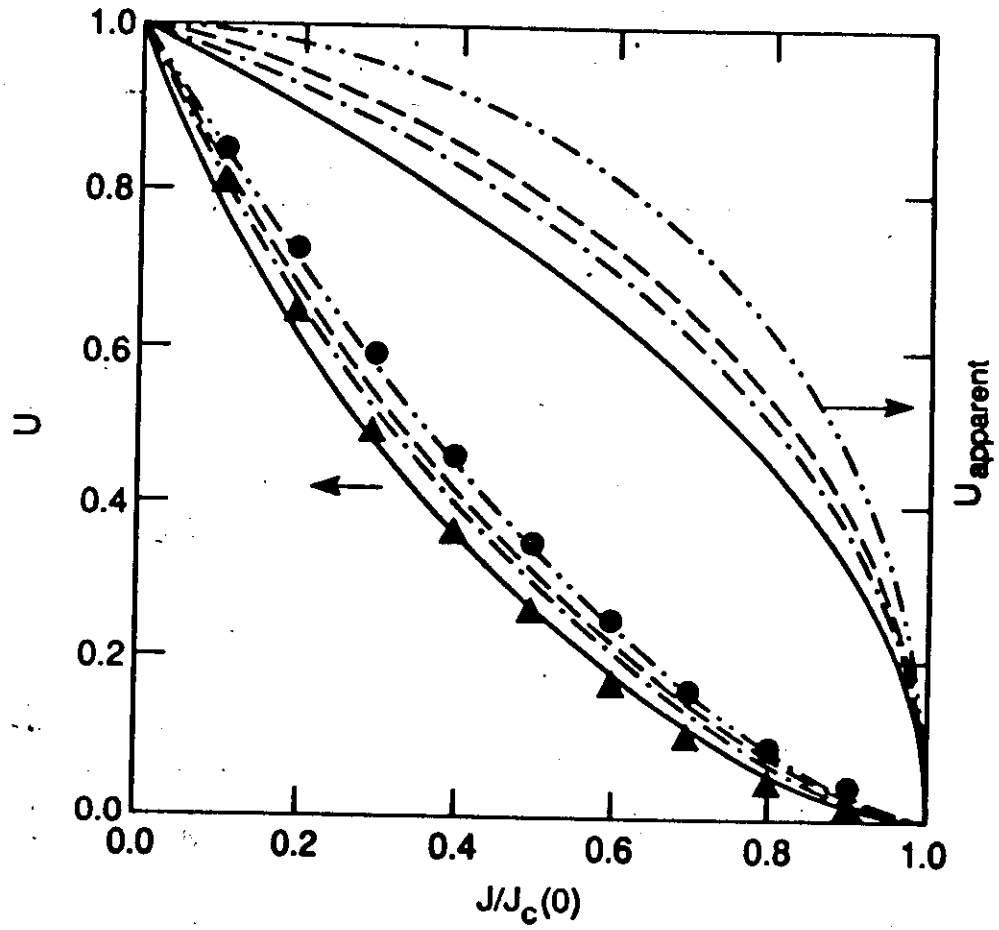

● $[1 - J/J_c(0)]^{3/2}$

▲ $[1 - J/J_c(0)]^{2}$

all continuous smooth potentials ——→ $(1 - J/J_c(0))^{3/2}$ asymptotically as $J \to J_c(0)$

THE "Beasley effect":

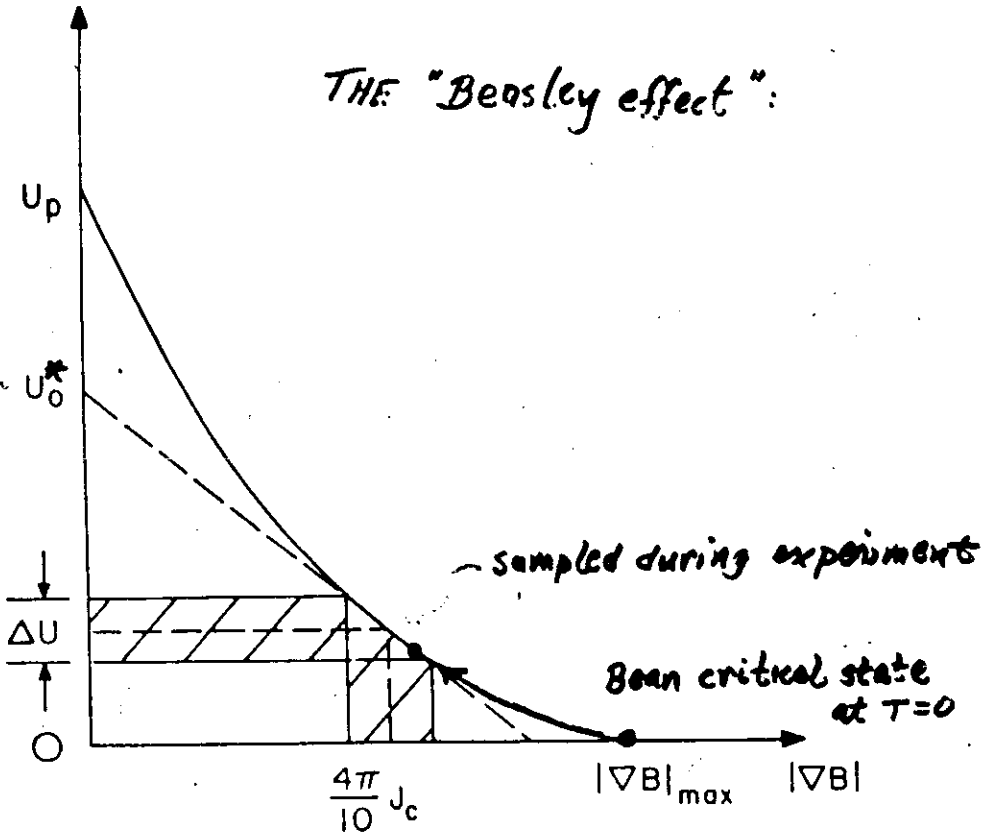

Fig. 1 (After Beasley et al.)

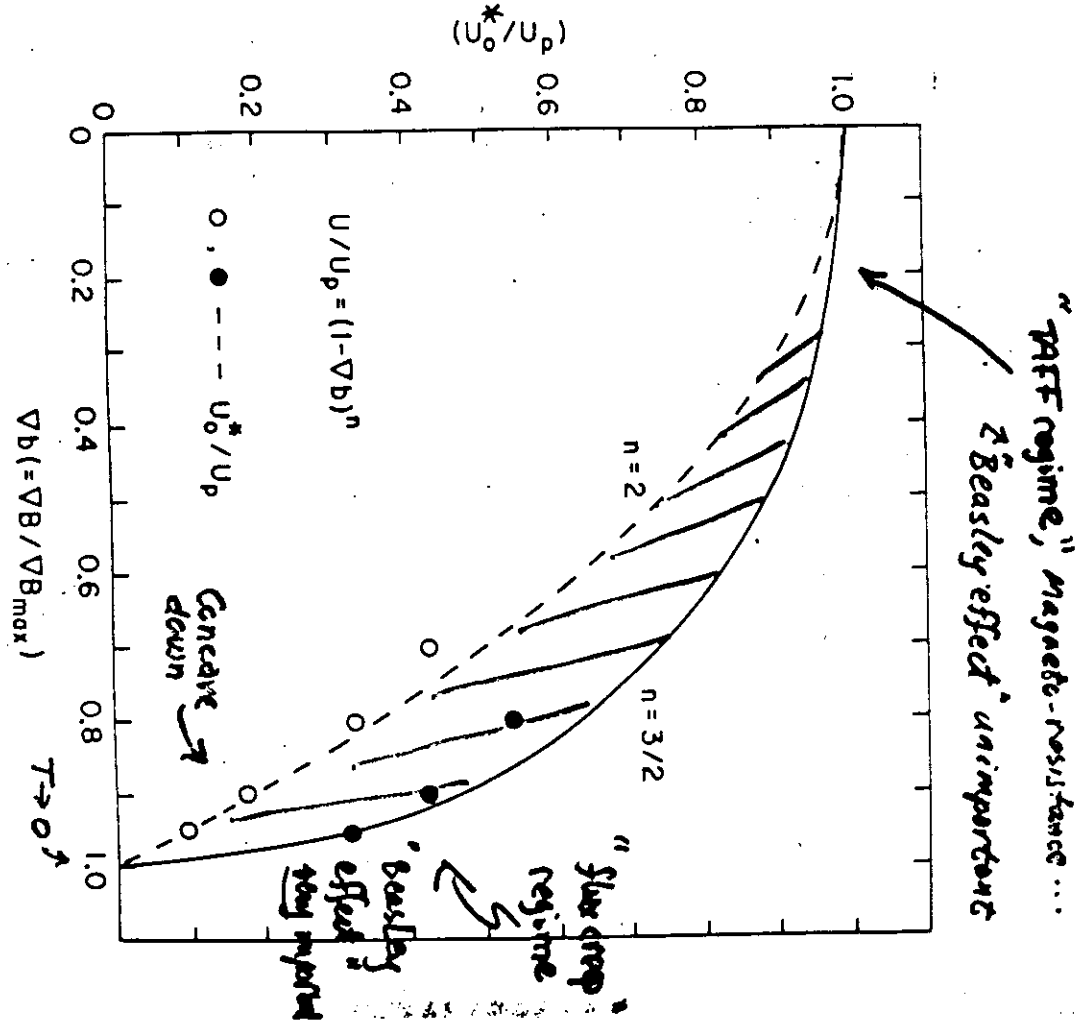

"TWO-WELL" MODEL of HAGEN, GRIESSEN AND SALOMONS (1989)

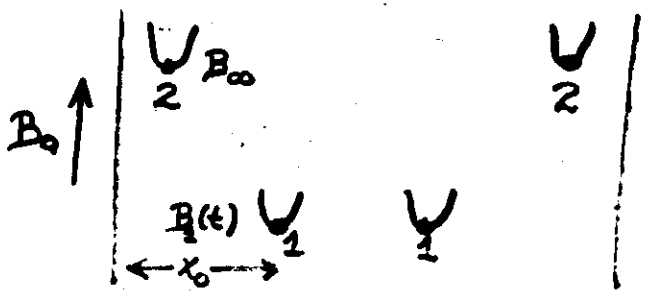

$$J = \frac{B_\infty - B_1}{2 x_0 \mu_0} \qquad \frac{M(t)}{M(0)} = \frac{B_\infty - B_1(t)}{B_\infty - B_1(0)}$$

$$\frac{dB_1}{dt} \simeq \tfrac{1}{2} \nu_0 B_\infty e^{-\Delta E_+ / KT}$$

$$\Delta E_+ = U_p \cdot \text{function}\left(\frac{J}{J_c}\right)$$

Welch, IEEE Trans. Magnetics ('91)

EXPLICIT CONSIDERATION OF VARIOUS TYPES OF POTENTIAL WELL LEADS TO :

$$\Delta E_+ \simeq U_p \left(1 - \frac{J}{J_c}\right)^n$$

with $\frac{3}{2} \lesssim n \lesssim 2$

($n=1$: Anderson approx.)

"Two-well" model of Hagen, Griessen, & Salomons leads to :

$$U_p \left(1 - \frac{J}{J_c}\right)^n \simeq U_p \left(\frac{B_1(t) - B_1(0)}{B_\infty - B_1(0)}\right)^n$$

$$\Downarrow$$

$$\int_0^{\left(\frac{U_p}{KT}\right)^{1/n} \frac{|\Delta M(t)|}{M_0}} e^{x^n} dx = \frac{t}{\tau_0} \cdot \frac{1}{\left(\frac{U_p}{KT}\right)^{1-\frac{1}{n}}}$$

when $n=1$: $\Delta M \propto \ln t$ after $t > \tau_c$

THEORETICAL CALCULATIONS OF
Effect of n, in $U = U_0(1 - T/T_c)^n$, on creep rate

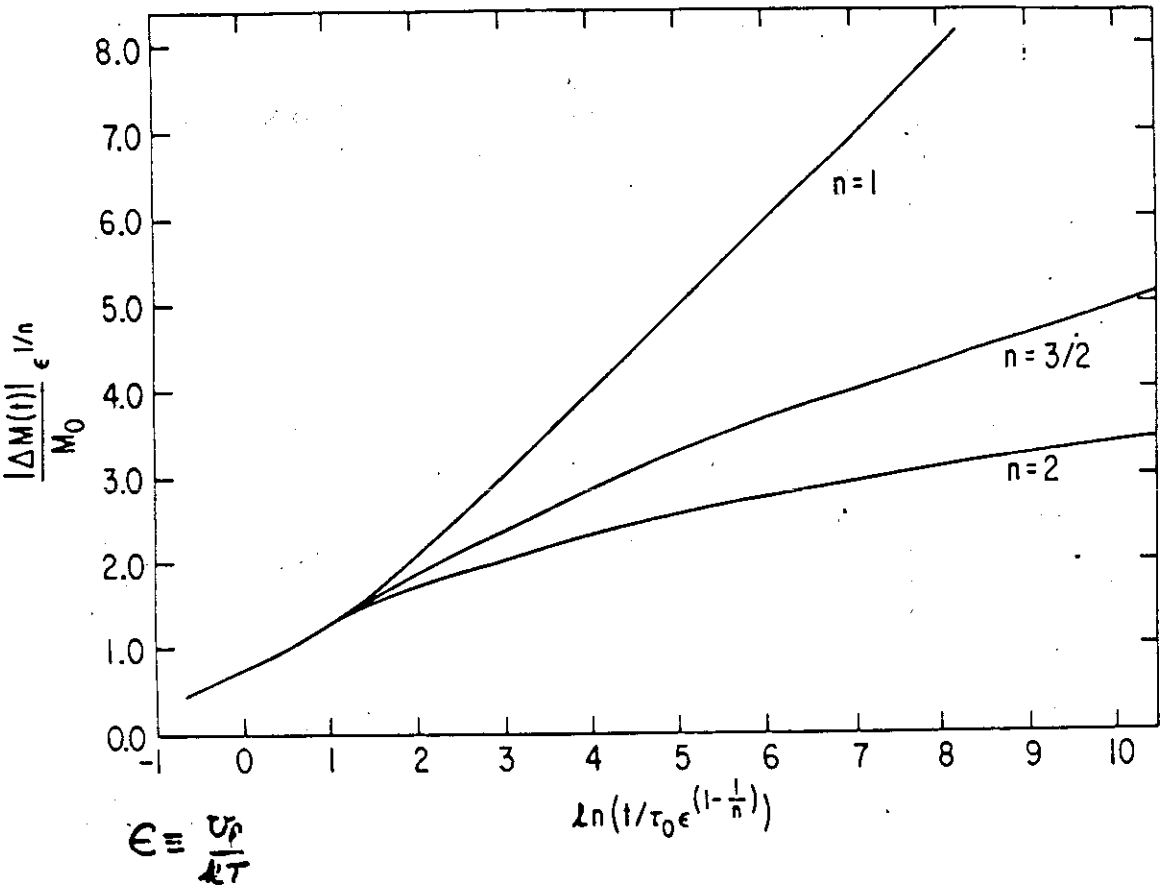

THEORETICAL Expectations, cont.

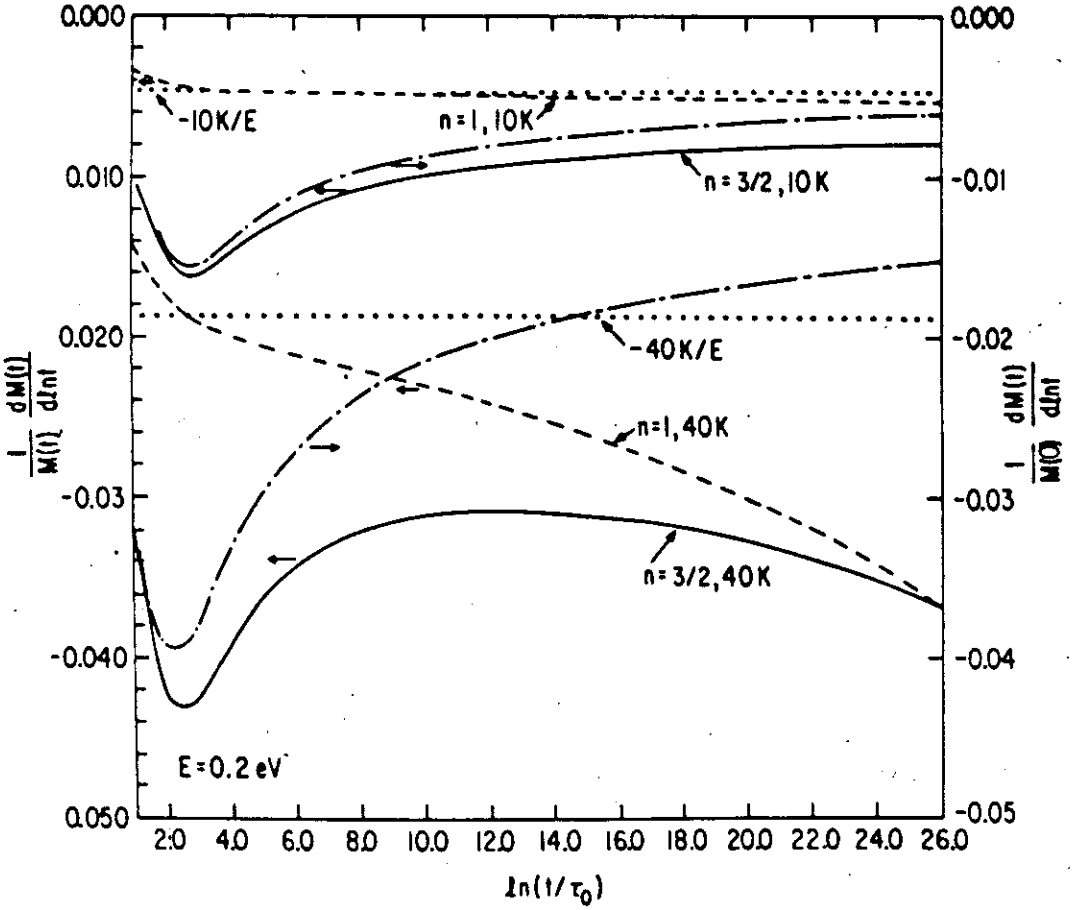

Comparison of these data with the previous transparency suggests $n > 1$

Melt-textured $YBa_2Cu_3O_x$ (from Nippon Steel)

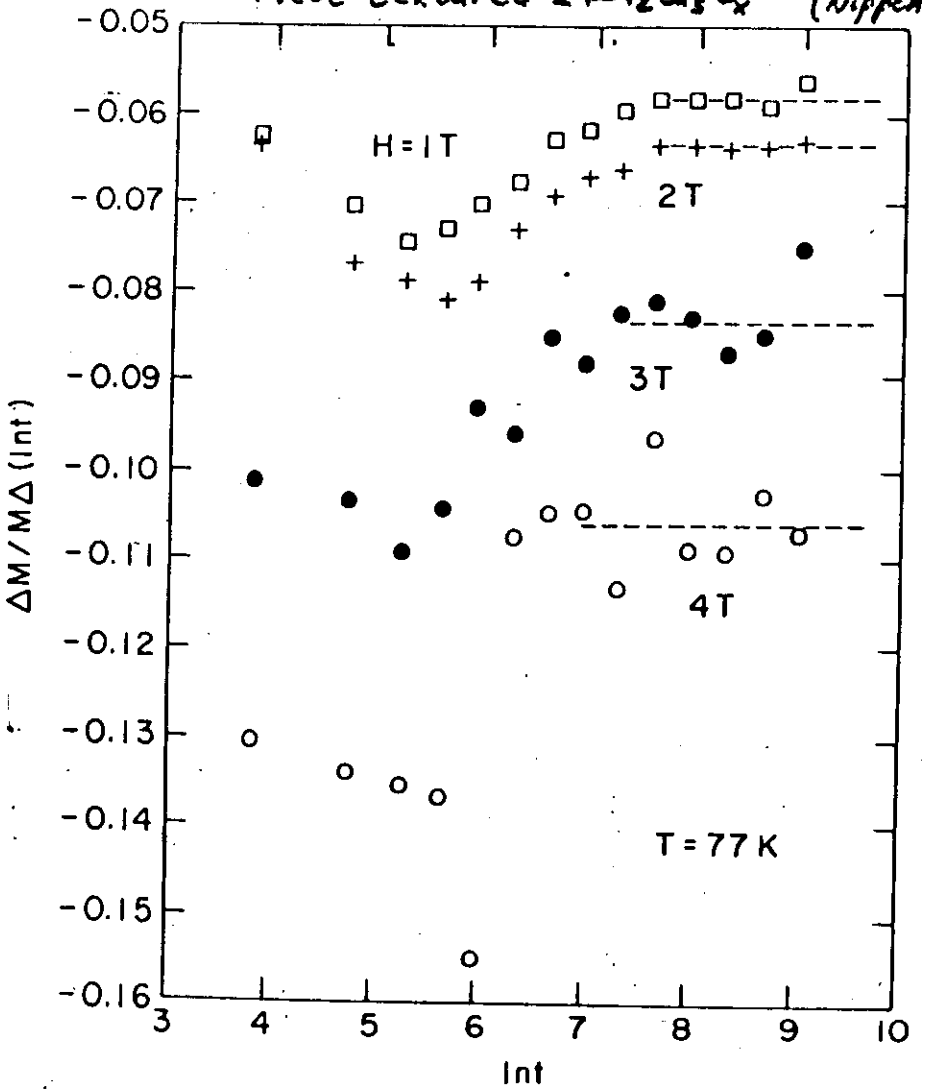

also see Xu, Suenaga, Moodenbaugh & Welch, Phys. Rev B (Dec 1, '89

ERRONEOUS T DEPENDENCE CAUSED BY ASSUMING n = 1

For general n:

Actual potential → $U_p = \dfrac{kT}{[c(n)\,|dM/dlat|_{max}]^n}$ $\left(\dfrac{}{M_0}\right)$

Assuming $n=1 \rightarrow U_0^*$ and ↓

Apparent potential → $U_0^* = c(n)\, U_p^{1/n}\, (kT)^{\frac{n-1}{n}}$

* When $n>1$ $\quad U_0^* \rightarrow 0$ as $T \rightarrow 0$

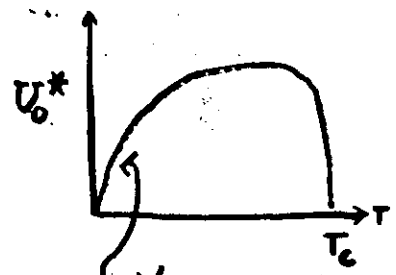

always concave downwards

but:

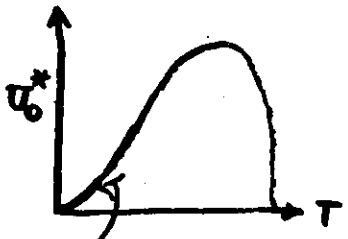

upward curvature caused by distribution of U_0's

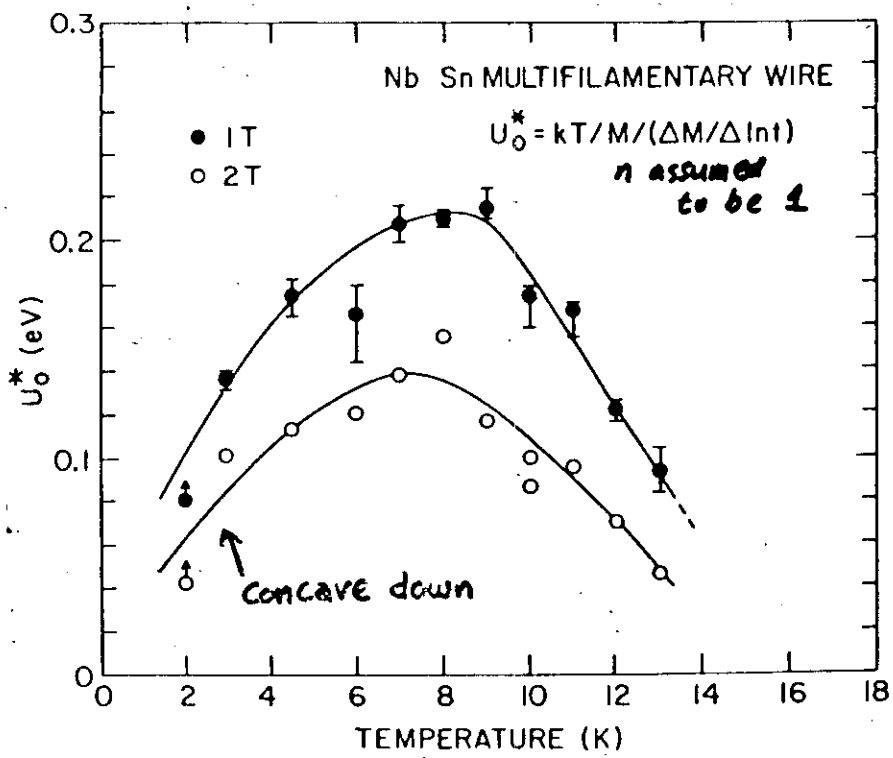

Probably caused by nonlinearity; Distribution of activation energies probably unimportant.

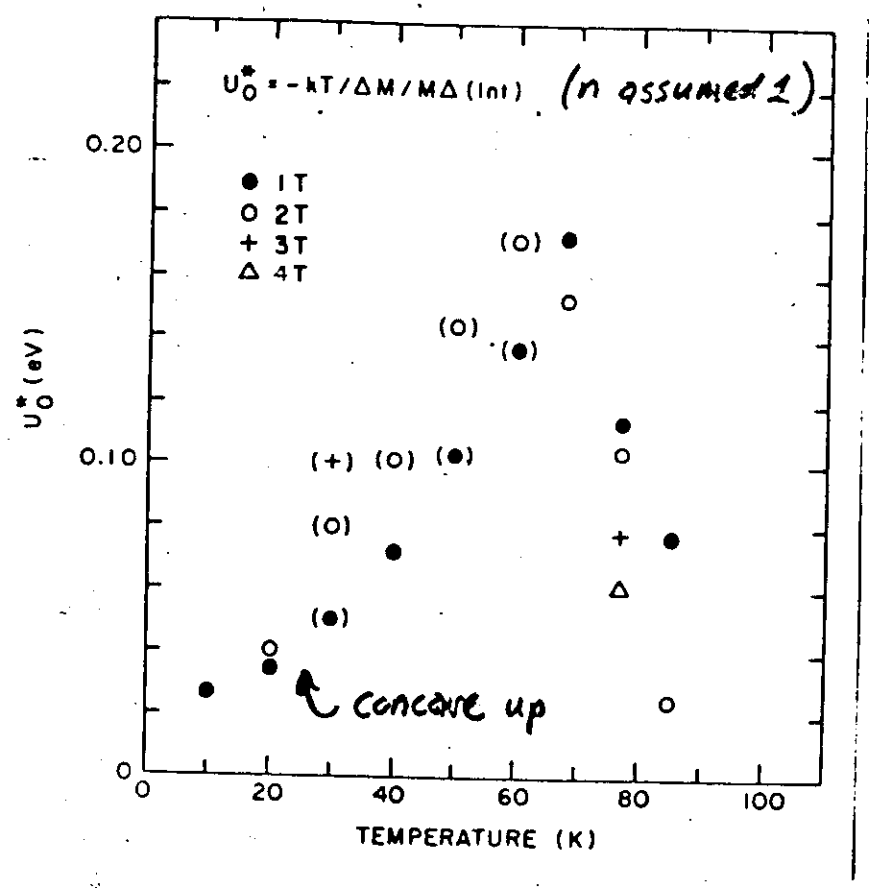

Fig. [illegible]: The temperature dependence of the apparent pinning potential U_0^* for a melt textured $YBa_2Cu_3O_7$.

probably caused by distribution of activation energies.

- INCORPORATING DISTRIBUTION OF U_p INTO SIMPLE "2-WELL" MODEL IS EASY.

EXAMPLE:

(percolation effects ignored)

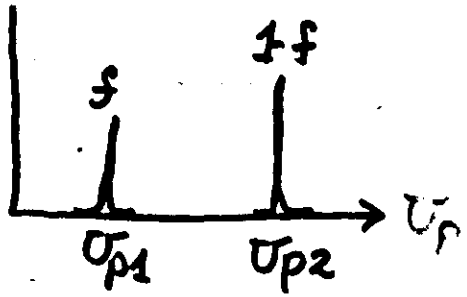

$$\int_0^{\epsilon^{1/n}|\Delta M(t)|/M_0} \frac{dx}{[f e^{-rx^n} + (1-f)e^{-x^n}]} = \frac{t}{\tau_0 \epsilon^{(1-1/n)}}$$

where $\epsilon \equiv U_{p2}/kT$ & $r = U_{p1}/U_{p2}$

CONCLUSION:

- Non-linearity in U vs J must be taken into account in order to obtain realistic values of the pinning energy and its spectral distribution from the analysis of magnetic flux creep data.

- A simple "2-well" model, adopted from that of Hagen et al., is easily used to approximate the effects of both non-linear $U(J)$ and a distribution of pinning properties.

The origin of magnetic field dependent resistive losses in high T_c thin film superconductors

Systems studied;

A. $Y_2Ba_4Cu_8O_{16}$ epitaxial thin films

T_c = 82.5 K, $J_c = 10^5$ A/cm^2 at 77 K

B. $Y_1Ba_2Cu_3O_7$ epitaxial films

T_c = 91 K , $J_c = 10^6$ A/cm^2 at 77k

Transport measurements;

1. Magnetoresistance
   (H, T and angular dependence)
2. Current - Voltage (I-V) characteristics
   (H, T and angular dependence)

CRITICAL CURRENT DENSITY
J-H-T Phase field.

Fig. 3 Field induced broadening of the resistive transition of a BiSSCO single crystal in both H// a-b and H⊥a-b configurations (Palstra et al Phys. Rev. Lett. 61, 1662 (1988)).

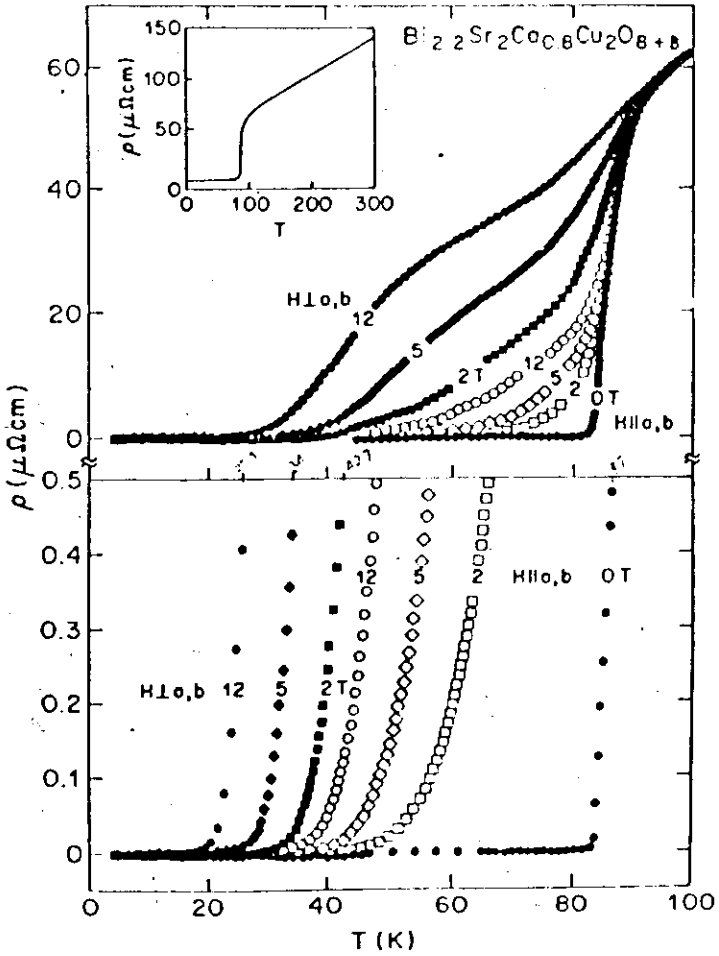

2-4-8 Film

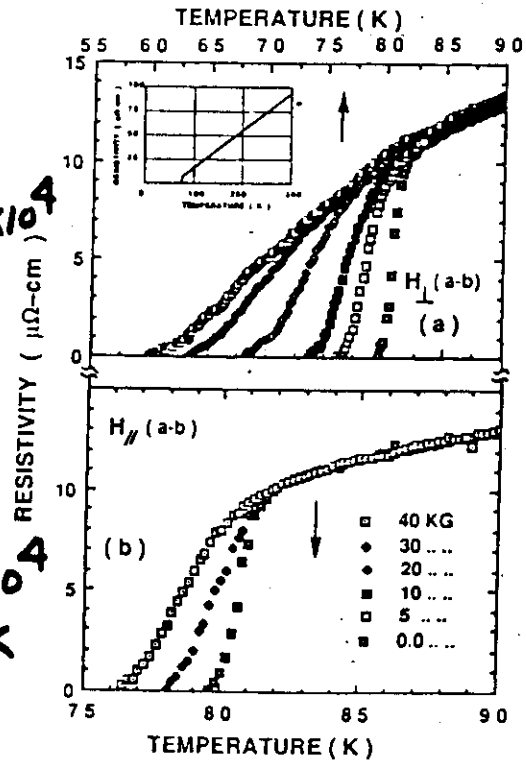

$\frac{dH_{c_2}}{dT} = -0.27 \times 10^4$ G/K

$H \perp a\text{-}b$

$J \perp H$

$\frac{dH_{c_2}}{dT} = -1.7 \times 10^4$ G/K

$H // a\text{-}b$

$J \perp H$

MEASUREMENT IN OHMIC REGIME; EXCITATION CURRENT DENSITY $\simeq 17 A/cm^2$.

Solid state Commun. 73, 337 (1990)

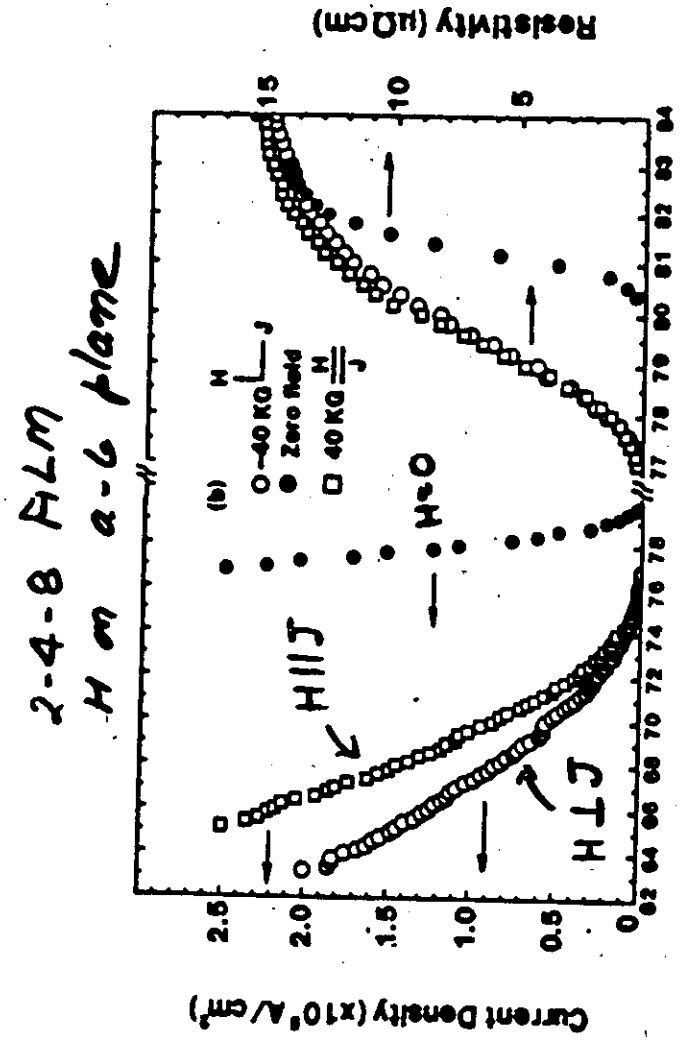

2-4-8 FILM
H in a-b plane

Phys. Rev. Lett. 64, 1666 (1990)
Fig. 1(b)
Oshimi et al.

CURRENT DEPENDENCE OF RESISTIVE TRANSITION. H & J on a-b plane.

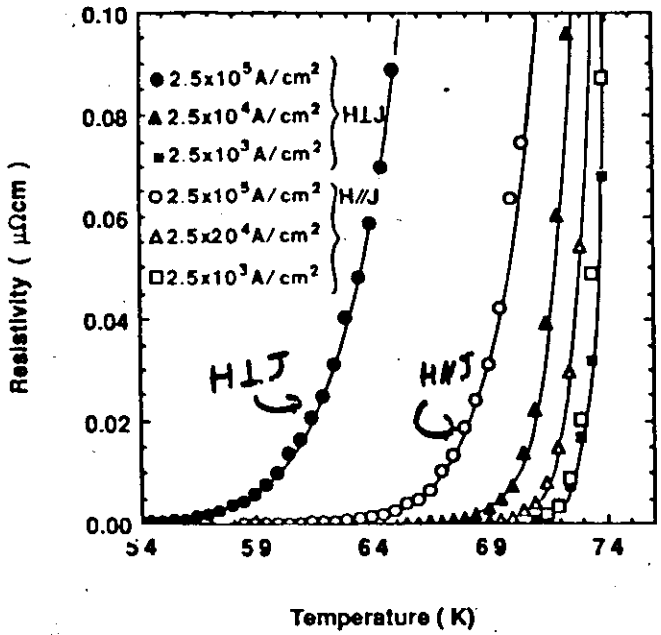

$Y_2 Ba_4Cu_8O_{16}$

Current dependence of the resistive transition in 1-2-3 film.

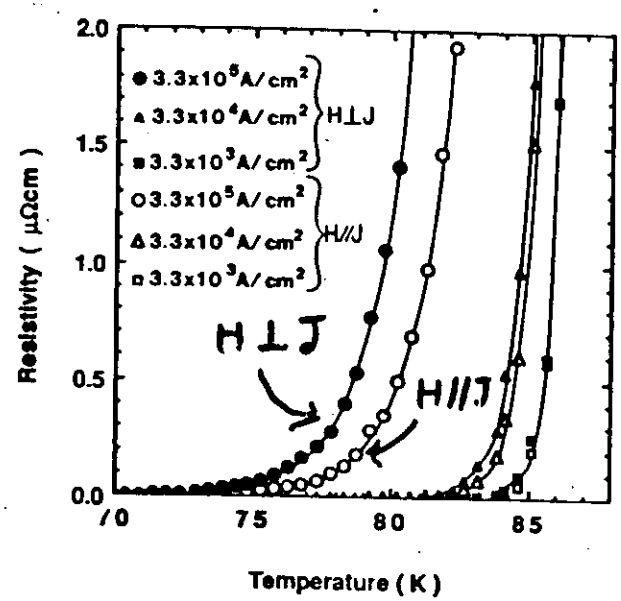

Field and current both in a-b plane.

Possible explanations for the force free dissipation

1. Crossing, entanglement and reconstruction of the flux lines may lead to a net transverse induction even in a nominal force free configuration. The transverse component would lead to a Lorentz force on the flux lines.

2. If the system has weak links and the transport is via Josephson coupling , thermal fluctuations may disrupt coupling of the phases of the order parameter. This would result in a thermally activated voltage in the force free configuration.

3. Thermodynamic fluctuations in the order parameter below the mean field temperature may cause formation of non-superconducting regions in the material. The size of such regions is dictated by the strength of the magnetic field.

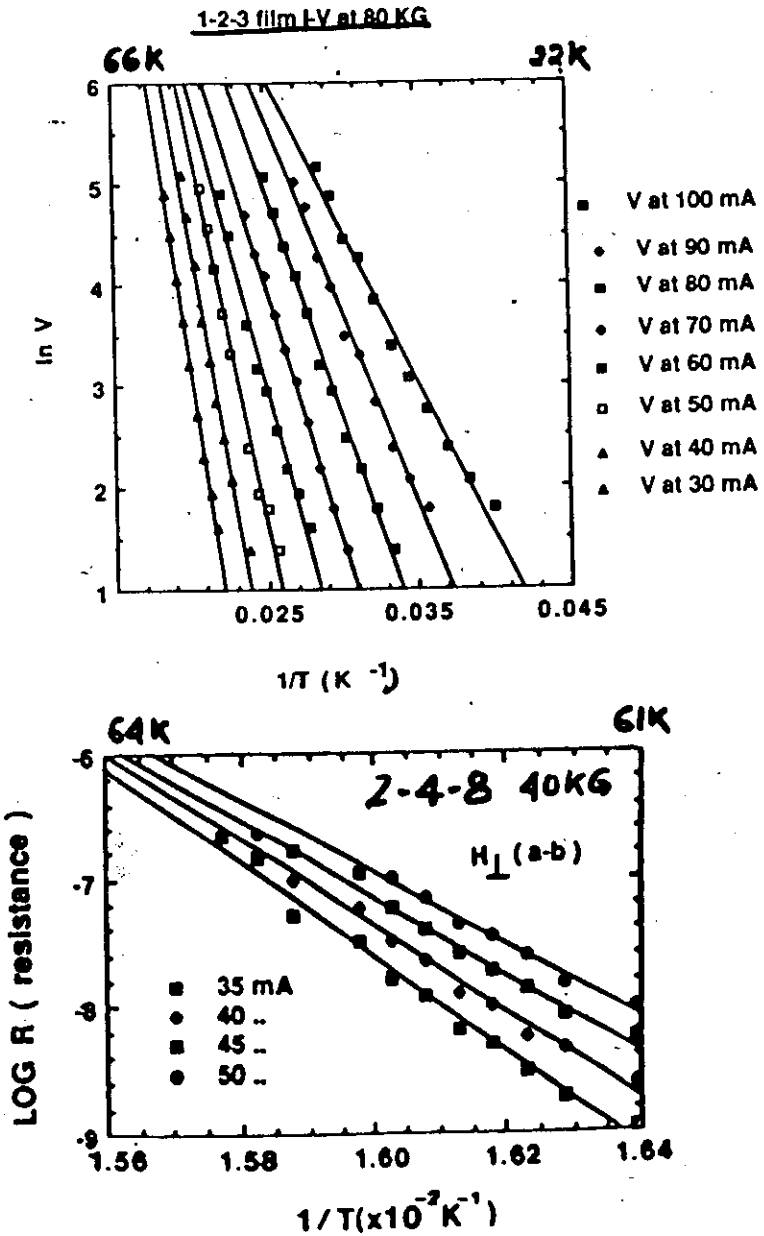

Conclusions

* For magnetic fields coplanar with transport current and CuO_2 sheets, (the nominal force free configuration) both 1-2-3 and 2-4-8 films show a significantly higher dissipation.

* At high transport current densities the effects the Lorentz-force are distinctly visible.

* Analysis of the thermally activated magnetoresistance in the framework of the standard flux creep theory, with a temperature and current dependent activation energy is possible.

* The flux pinning potential in 1-2-3, deduced from such analysis is twice as large as for 2-4-8. This observation emphasizes the role of c_{44} in these layered superconductors.

Badhani et al.,
Phys. Rev. Lett. 64 (1990)

DO FLUX-LINE LATTICES IN SUPERCONDUCTORS MELT?

- Several groups have found for oxide superconductors (HTSCs) that:

  Magnetic flux lines move <u>reversibly</u> when acted on by the Lorentz force if:

  $$T > T_{irr}(H)$$

  and it has been proposed that $T_{irr} = T_{melting\ point}$

  If so, there may be <u>intrinsic</u> reasons for giant flux creep and low critical current densities in HTSCs at high T.

- A systematic study of $T_{irr}(H)$ for both HTSCs and the conventional superconductors (LTSCs) Nb, Nb-Ti, and Nb_3Sn at BNL has shown that:

  - a substantial region of reversible flux motion in the H-T plane exists for LTSCs as well as HTSCs
  - T_{irr} for HTSCs is probably a consequence of thermally-activated depinning and not melting
  - for LTSCs, T_{irr} probably <u>is</u> a flux-lattice melting temperature

- Significance

  T_{irr} in HTSCs is not an intrinsic property and can probably be raised substantially by the addition of suitable pinning centers.

<u>Performers:</u> M. Suenaga, Y. Xu, A. Ghosh, and D. O. Welch, Brookhaven National Laboratory.

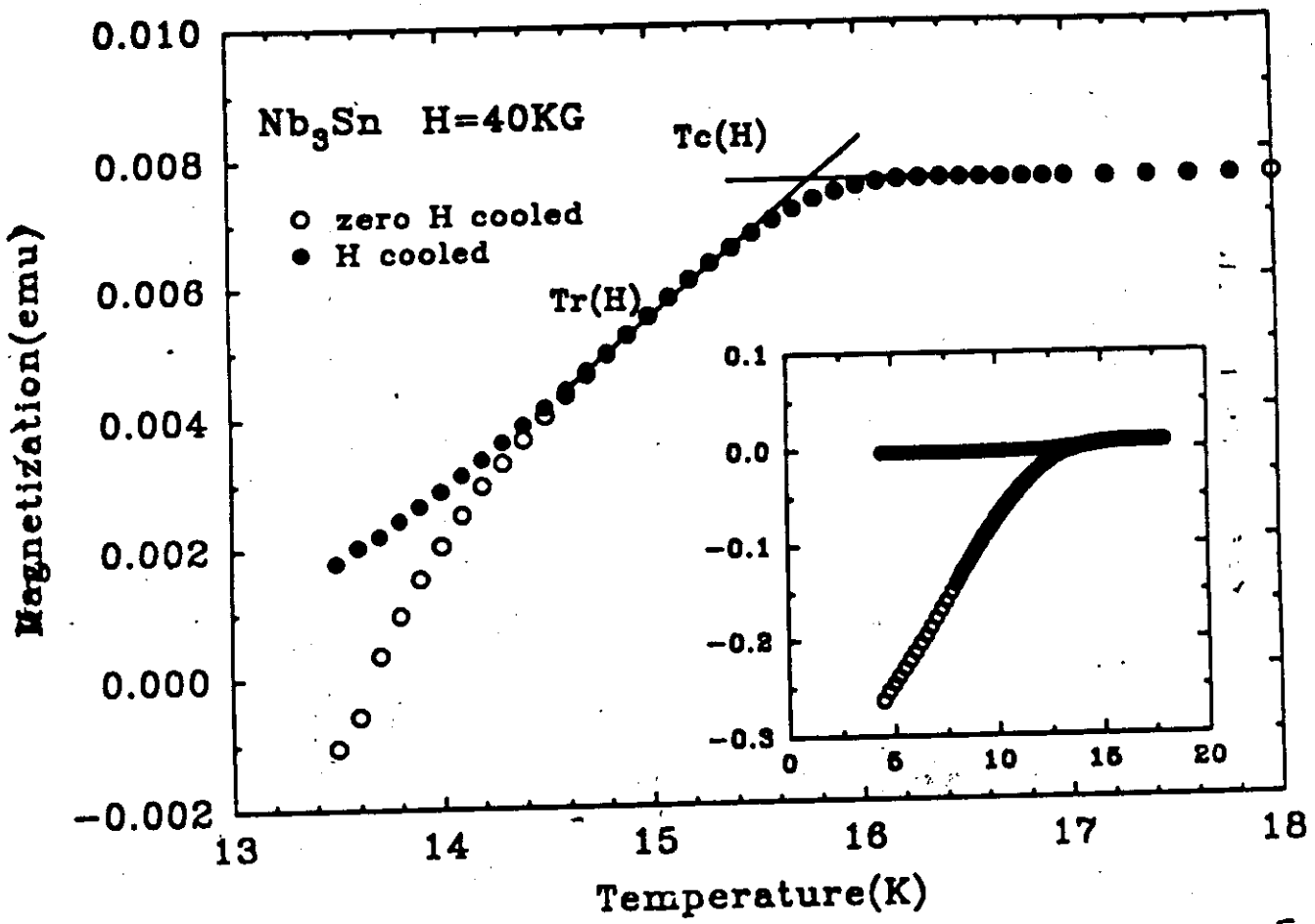
Nb3Sn H=40KG
Tc(H)
Tr(H)
zero H cooled
H cooled
Magnetization(emu)
Temperature(K)
0.010
0.008
0.006
0.004
0.002
0.000
−0.002
13
14
15
16
17
18
0.1
0.0
−0.1
−0.2
−0.3
0
5
10
15
20

Fig. 1

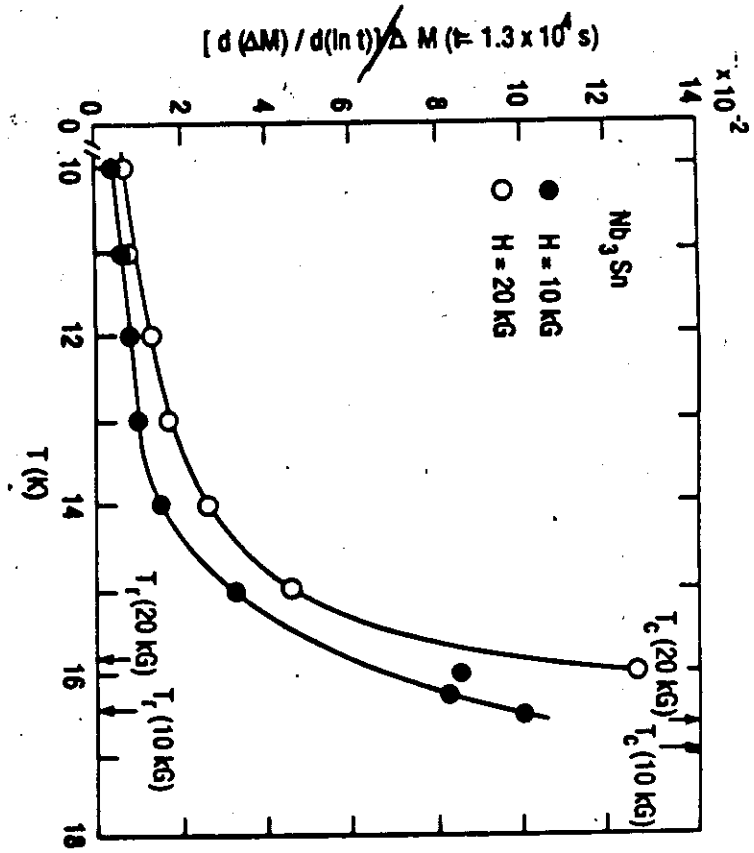
[d(ΔM)/d(ln t)]/ΔM (t= 1.3 x 10⁴ s)
x10⁻²
0
2
4
6
8
10
12
14
T (K)
10
12
14
16
18
Nb3Sn
H = 10 kG
H = 20 kG
Tr (20 kG)
Tr (10 kG)
Tc (20 kG)
Tc (10 kG)

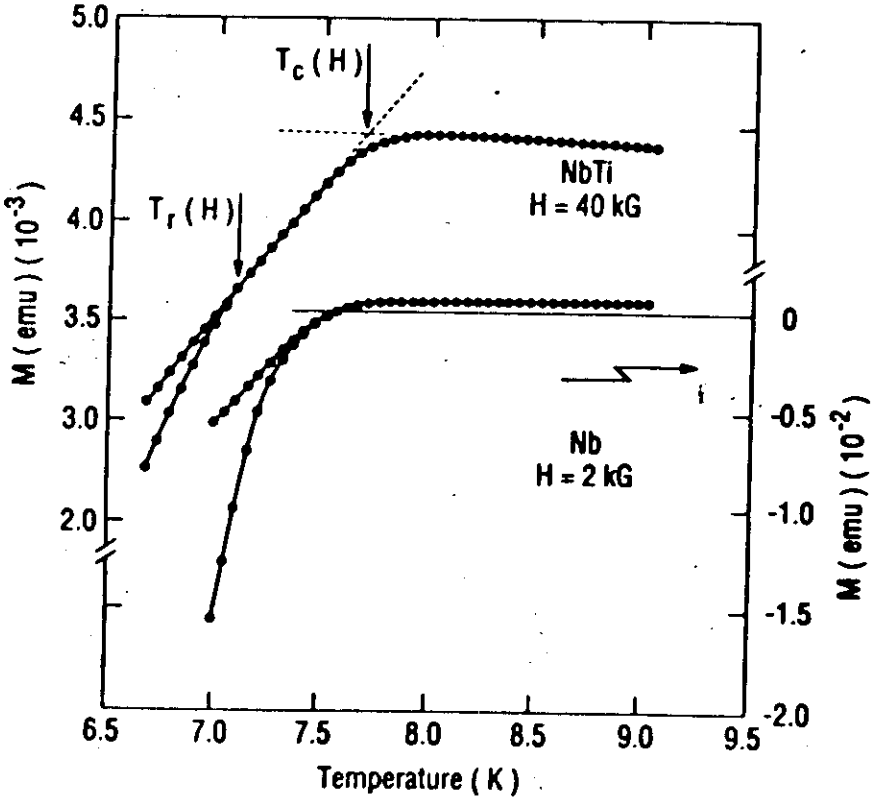

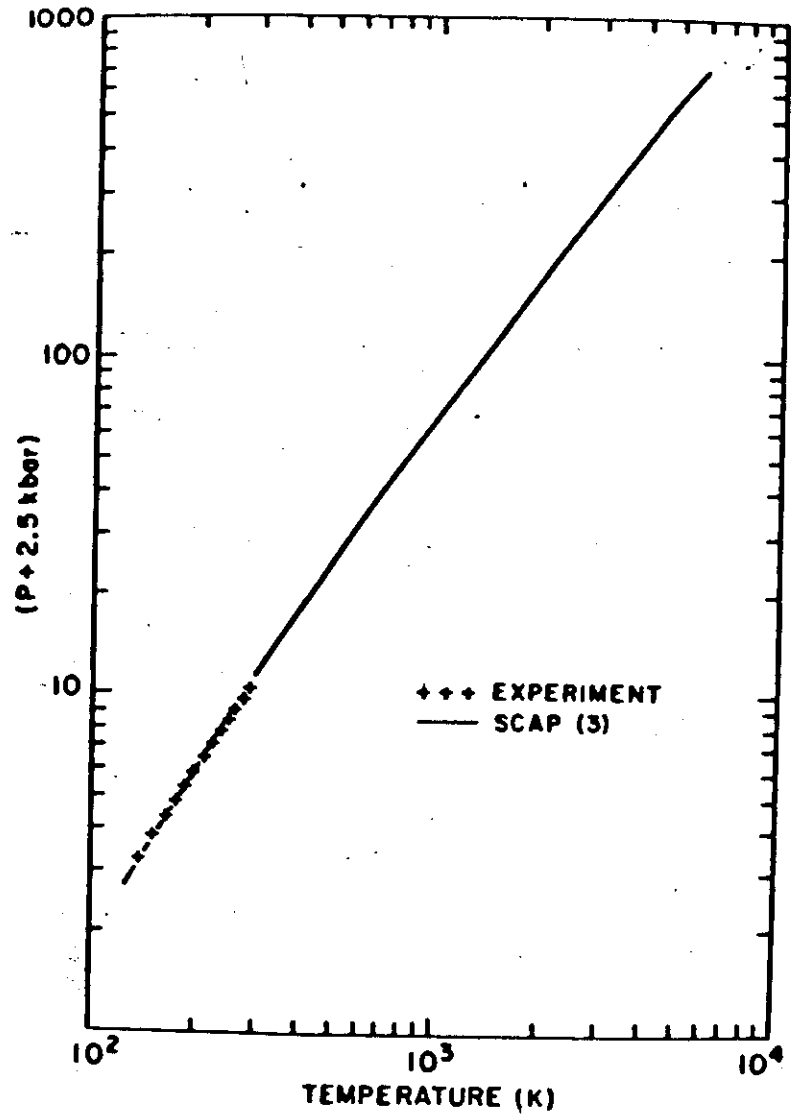

FIG. 15. A comparison of the pressure along the melting curve for Kr with theory. The pressure plus 2.5 kbar is plotted verus the melting temperature. The experimental data are from Ref. 15.

Atomic melting Lindemann "law"

Low-T_c Superconductor, Nb-Ti

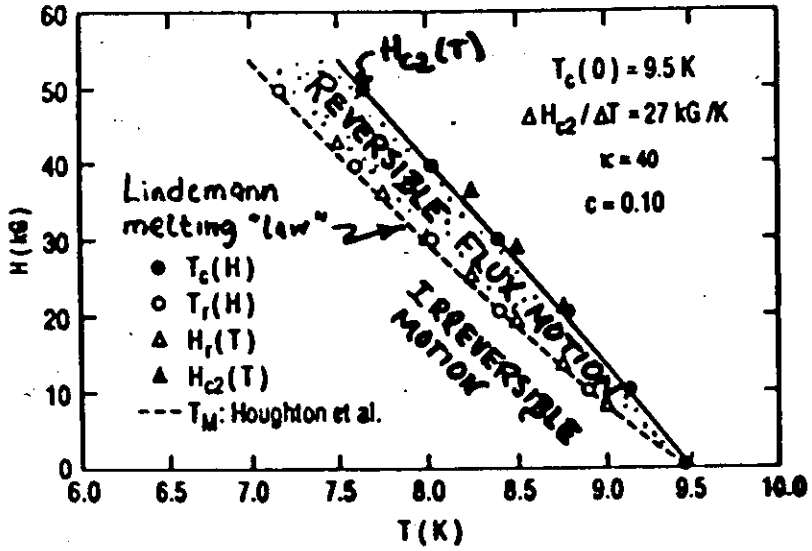

The transition from irreversible to reversible flux-line motion in this low-T_c superconductor is probably caused by the melting of the flux-line lattice.

(Suenaga et al., '90)

Fig. 2

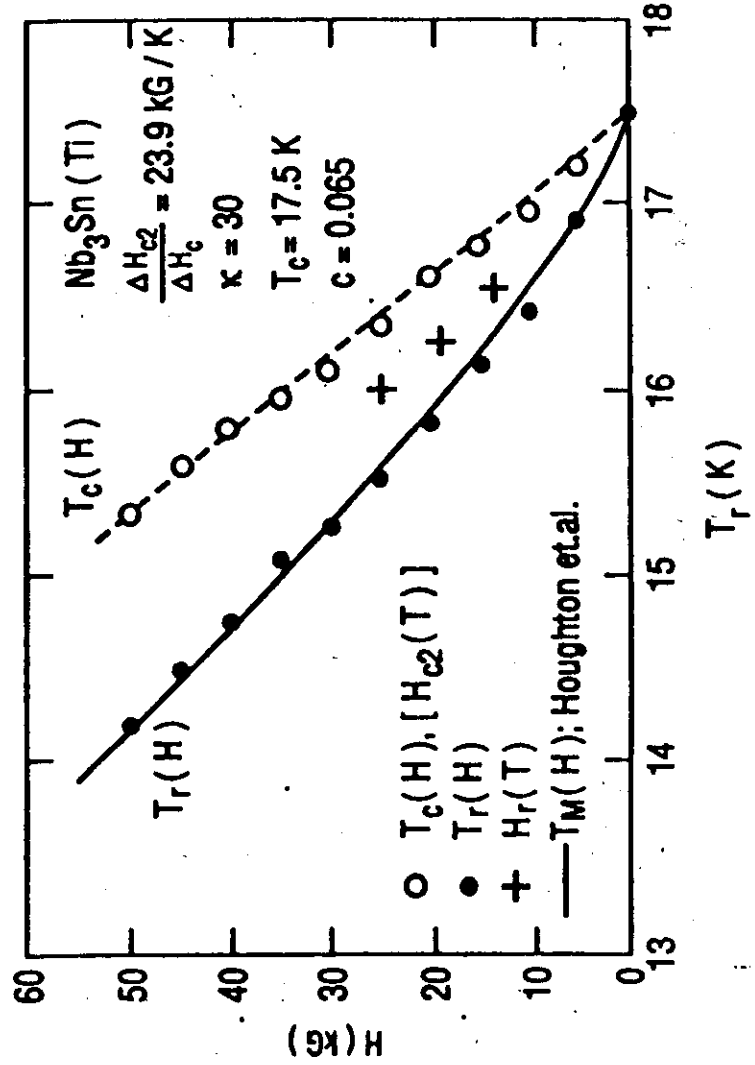

High-T_c Bi-Cuprate Superconductors

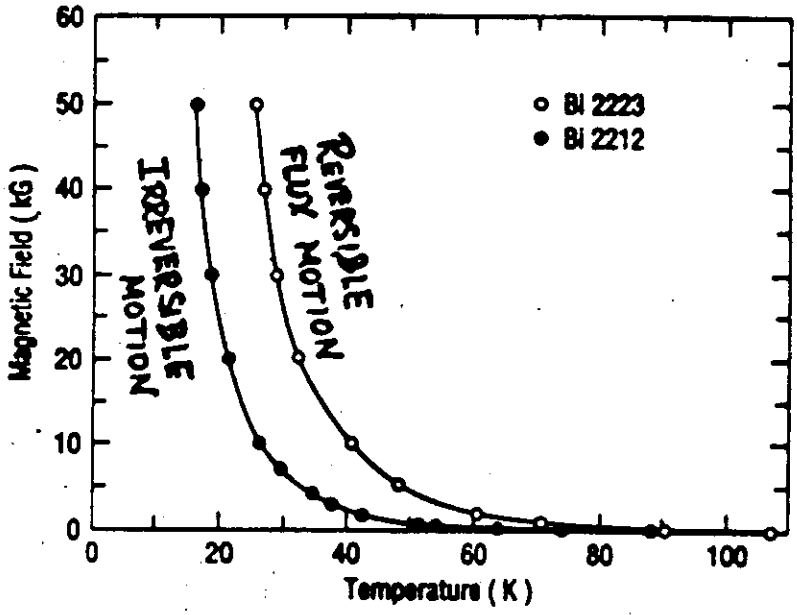

(Suenaga et al. '90)

The transition from irreversible to reversible flux-line motion in these high-T_c superconductors is probably caused by thermally-activated depinning. Therefore improved pinning can raise the transition temperature and thus increase usable range.